N-Methyl-D-aspartate receptor hypofunction causes recurrent and transient failures of perceptual inference

Authors:

Veith Weilnhammer[1,2,3,ec], Marcus Rothkirch[1,4,ec], Deniz Yilmaz[1,5,6,7,ec], Merve Fritsch[1], Lena Esther Ptasczynski[1,5], Katrin Reichenbach[1], Lukas Rödiger[1], Philip Corlett[8], Philipp Sterzer[9]

Affiliations:

[1] Department of Psychiatry, Charité-Universitätsmedizin Berlin, corporate member of Freie Universität Berlin and Humboldt-Universität zu Berlin, Germany
[2] Berlin Institute of Health, Charité-Universitätsmedizin Berlin and Max Delbrück Center, Germany
[3] Helen Wills Neuroscience Institute, University of California Berkeley, USA
[4] Medical School Berlin, Hochschule für Gesundheit und Medizin, Germany
[5] Berlin School of Mind and Brain, Humboldt-Universität zu Berlin, Germany
[6] Max Planck School of Cognition, Leipzig, Germany
[7] Department of Psychiatry and Psychotherapy, LMU University Hospital, Munich, Germany
[8] Department of Psychiatry, Yale University School of Medicine, New Haven, USA
[9] Department of Psychiatry (UPK), University of Basel, Switzerland

Contributions:

[ec] Equal contribution

Corresponding Author:

Veith Weilnhammer, Helen Wills Neuroscience Institute, University of California Berkeley, USA, email: veith.weilnhammer@gmail.com

Running Title: Failures of inference under ketamine

Keywords: schizophrenia, psychosis, ketamine, predictive processing, bistable perception, modes of inference

1 Abstract

Perception integrates external sensory signals with internal predictions that reflect prior knowledge about the world. Previous research suggests that this integration is governed by slow alternations between an external mode, driven by sensory signals, and an internal mode, shaped by prior knowledge. Using a double-blind, placebo-controlled, cross-over experiment in healthy human participants, we investigated the effects of the N-Methyl-D-aspartate receptor (NMDAR) antagonist S-ketamine on the balance between external and internal modes. We found that S-ketamine causes a shift of perception toward the external mode. A case-control study revealed that individuals with paranoid Scz, a disorder repeatedly associated with NMDAR hypofunction, spend more time in the external mode. This NMDAR-dependent increase in the external mode suggests that the symptoms of schizophrenia are caused by recurring dissociations of perception from prior knowledge about the world.

2 Introduction

Imagine a dimly lit room at a crowded party, where unclear visual signals, indistinct sounds, and complex social interactions allow for multiple - and sometimes false - interpretations. In such ambiguity, failures of perceptual inference, the ability to contextualize sensory inputs with prior knowledge about the world, can lead to profound departures from reality: Faces obscured in shadow may appear distorted, random noise could be perceived as a whisper, and friendly smiles might seem derogatory.

According to the canonical predictive processing hypothesis[1], a disruption of perceptual inference is likely to play a crucial role in schizophrenia (Scz), a severe mental disorder characterized by psychotic symptoms such as delusions and hallucinations[1]. People with Scz may fail to apply prior knowledge to the interpretation of ambiguous sensory signals, causing erratic inferences that lead to hallucinatory experiences and delusional beliefs[1]. Yet despite considerable progress in the computational understanding of psychosis, two key questions have remained unanswered.

The first question concerns the neural mechanisms that cause perceptual inference to fail in Scz. Formal predictive processing accounts of Scz foreground the role of prediction errors in updating Bayesian beliefs about the causes of sensory input[2]. Most accounts focus on a failure to predict or instantiate the precision afforded to prediction errors at various levels of the cortical hierarchy[1]. Precision refers to the confidence ascribed to prediction errors, and regulates how prior expectations are updated in response to sensory information[2].

Mathematically, precision is equivalent to the (Kalman) gain or the weighting of prediction errors in predictive processing models of perceptual inference[3]. Psychologically, the deployment of sensory precision can be understood in terms of selective attention (or sensory attenuation)[4]. Physiologically, precision corresponds to the postsynaptic gain or excitability of neuronal populations that report prediction errors, commonly mediated by N-Methyl-D-aspartate receptors[5] (NMDARs).

Beyond predictive processing theory, several lines of evidence point to NMDAR hypofunction as a key factor in the pathophysiology of psychosis[6]. NMDAR antibodies[7] and antagonists such as ketamine[8] mimic the symptoms of Scz, which is itself associated with a reduction of NMDAR density in the prefrontal cortex[9]. In addition to their role in controlling the excitability of prediction error neurons[6] and their general function for maintaining the cortical excitation-inhibition balance[10], NMDARs play a critical role in cortical feedback[11], support synaptic short-term plasticity[12], and interact with neuromodulators such as dopamine and serotonin via GABAergic interneurons[13]. While these NMDAR-dependent mechanisms are likely critical for perceptual inference, it is yet to be determined how NMDAR hypofunction may cause the symptoms of Scz.

The second unresolved question concerns the temporal dynamics of psychotic experiences, which often unfold as short-lived events spanning from seconds to minutes, especially at early stages of Scz. The transient nature of psychotic experiences challenges models that assume a constant disruption of perceptual inference[1]. A solution to this problem is suggested by the recent observation that perceptual inference is subject to spontaneous fluctuations over time[14]. Such fluctuations have been related to two opposing modes of inference, or shifts in attentional sets, during which perception is driven predominantly either by external inputs (external mode) or by internal predictions that stem from recent experiences[15] (internal mode, Figure 1A). Although preliminary evidence indicates a tendency toward the external mode in people with Scz[16], the neural mechanisms of mode fluctuations and their potential implications for computational models of Scz have remained elusive.

The objective of the current study was therefore twofold: First, to test whether NMDAR hypofunction causes changes in perceptual inference that characterize Scz; and second, to explore the effect of NMDAR hypofunction on ongoing fluctuations in perceptual inference that may explain the transient nature of psychotic experiences. We addressed these questions in a double-blind, placebo-controlled, cross-over experiment with S-ketamine in healthy participants, and a case-control study that compared patients with paranoid Scz to matched healthy controls[17]. Participants engaged in a task designed to test how internal predictions derived from previous experiences modulate the perception of sensory signals that varied in

ambiguity. We found that NMDAR antagonism and Scz were associated with a shift of perception toward the external mode, a minute-long state of the brain during which inference dissociates from prior knowledge. Our results suggest that NMDAR hypofunction shifts the balance between external and internal modes, and may thus contribute to the symptoms of Scz by causing transient and recurring failures of perceptual inference.

3 Materials and Methods

For details on the experimental paradigm, participant recruitment and consent, inclusion/exclusion criteria, randomization and blinding, drug administration protocols, safety monitoring, data analysis, and computational modeling, please refer to Supplemental Methods S1.

4 Results

To investigate whether NMDAR hypofunction influences perceptual inference, and how NMDAR hypofunction contributes to the transient nature of psychotic experiences, we conducted a double-blind placebo-controlled cross-over experiment in 28 healthy human participants. The participants attended two experimental sessions during which they received a continuous intravenous infusion of either the NMDAR antagonist S-ketamine at a dose of 0.1 mg/kg/h or a saline placebo. In each session, the participants viewed ten 120 sec blocks of an ambiguous structure-from-motion (SFM) stimulus that induced the experience of a sphere rotating around a vertical axis, and reported changes in the perceived direction of rotation (leftward vs. rightward movement of the front surface) as well as their confidence in the choice (Figure 1B and Supplemental Video S1).

The ambiguity of the display induced the phenomenon of bistable perception: Even though the stimulus was physically ambiguous at each frame of the presentation, spontaneous changes in the perceived direction of rotation occurred in average intervals of 13.75 ± 3.09 sec. In line with previous results[17,18], these changes in perception occurred with a probability of $0.11 \pm 8.67 \times 10^{-3}$ at brief depth-symmetric configurations of the stimulus (see Supplemental Video S1 and Supplemental Figure S2A). We therefore divided the continuous behavioral reports into a sequence of discrete states t. Each state was associated with a perceptual experience y_t, confidence c_t and the external input s_t.

Predictive processing conceptualizes bistable perception as an inferential process about the cause of s_t. The core idea is that previous experiences (y_{t-1}) generate internal predictions that bias the interpretation y_t of the ambiguous stimulus[18] (Figure 1C). In this view, inferences during bistability mirror the temporal autocorrelation of natural environments, where the recent past typically predicts the near future, much like frames captured by a video camera allow for the prediction of future frames[19]. The adaptive benefit of this predictive strategy is the stabilization of perception that prevents erratic experiences in natural environments, which are highly autocorrelated and accessible to the brain only via inherently ambiguous sensory signals[2].

Predictive processing models of bistable perception assume that transitions between the alternative interpretations of (partially) ambiguous stimuli are driven by conflicts between the external input and stabilizing internal predictions[17,18]. To test how NMDAR antagonism alters the balance between external inputs and internal predictions, we attached a 3D signal to a fraction of the stimulus dots. The signal-to-ambiguity ratio (SAR) ranged from complete ambiguity to full disambiguation across five levels and remained constant in each block of the experiment. By changing the direction of rotation enforced by the 3D signal at random in average intervals of 10 sec, we created dynamic conflicts between the SAR-weighted input s_t and the stabilizing internal prediction y_{t-1}. Due to the random changes in s_t, a shift of inference away from internal predictions and toward external sensory data, which has repeatedly been associated with NMDAR hypofunction[1] and may be maladaptive in autocorrelated natural environments[15], should manifest as an increase in perceptual accuracy in our experiment.

4.1 NMADR hypofunction shifts perceptual inference toward the external input and away from internal predictions

As expected, we found that y_t was driven by both s_t ($\beta = 3.01 \pm 0.06$, z = 50.39, p = 0) and y_{t-1} ($\beta = 2.06 \pm 0.03$, z = 80.58, p = 0). Importantly, S-ketamine caused perception to shift toward s_t ($\beta = 0.45 \pm 0.08$, z = 5.6, $p = 1.71 \times 10^{-7}$, Figure 2A and Supplemental Figure S3), indicating a stronger weighting of external inputs over internal predictions during pharmacologically induced NMDAR hypofunction. Under the predictive processing formulation of perceptual inference, one can read the estimates for s_t and y_{t-1} as sensory and prior precision, respectively. This suggests that S-ketamine augments sensory precision by altering the interactions between pyramidal cells and fast-spiking inhibitory interneurons thought to underwrite cortical gain control or excitation-inhibition balance[10].

Next, we performed the same analysis on data from a previous case-control study using an analogous task in patients with Scz[17]. In Scz patients and controls, y_t was influenced by the SAR-weighted input s_t ($\beta = 2.77 \pm 0.11$, z $= -24.85$, p $= 2.18 \times 10^{-135}$) and the stabilizing prediction y_{t-1} ($\beta = 1.5 \pm 0.03$, z $= -58.2$, p $= 0$). Similar to S-ketamine, s_t had a larger impact on perception in Scz patients than controls ($\beta = 0.75 \pm 0.15$, z $= 4.96$, p $= 5.6 \times 10^{-6}$, Figure 2E and Supplemental Figure S4).

Together, these results align with the canonical predictive processing theory of Scz[1]: Pharmacologically-induced NMDAR hypofunction and Scz are associated with a shift of perceptual inference toward external inputs, and away from stabilizing internal predictions. This increase in sensory precision (relative to prior precision) is often framed as a failure of sensory attenuation, i.e., the inability to attenuate sensory precision or, psychologically, ignore unclear or irrelevant sensations[20]. In the artificial setting of our experiment, where stimuli are random, weak internal predictions under S-ketamine and in Scz lead to *increased* perceptual accuracy. In autocorrelated natural environments, however, NMDAR hypofunction may trigger psychotic experiences by causing erratic inferences about ambiguous sensory information.

4.2 NMDAR-dependent changes of perceptual inference stem from an altered balance between external and internal modes of perception

As a mechanism for symptoms that are transient and recurring, NMDAR-dependent changes in perceptual inference should not be constant, but fluctuate dynamically at a timescale that is compatible with the duration of individual psychotic experiences. We tested this prediction in Hidden Markov Models (HMM) that inferred transitions between two latent states, each linked to an independent general linear model (GLM) that predicted y_t from s_t and y_{t-1}. The β weights quantified the sensitivity to ambiguous sensory information ($\beta_S \times s_t$) relative to the stabilizing effect of internal predictions provided by preceding experiences ($\beta_P \times y_{t-1}$), and allowed us to evaluate dynamic changes in the balance $\Delta_{S-P} = \beta_S - \beta_P$ between the two.

Consistent with recent findings in humans and mice[14,15], Bayesian model comparison indicated a clear superiority of the two-state GLM-HMM over the standard one-state GLM in the S-ketamine experiment ($\delta_{BIC} = -3.65 \times 10^3$). According to the two-state GLM-HMM, perception fluctuated between an internal mode, shaped by the stabilizing internal prediction y_{t-1}, and an external mode, dominated by the SAR-weighted input s_t. External mode

increased Δ_{S-P} by 2.8 ± 0.29 (T(81) = 9.5, p = 5.22×10^{-13}, Figure 2B-C). Switches between modes occurred in intervals of 179.97 ± 19.39 sec.

The presence of slow fluctuations between external and internal modes suggests that, instead of causing a constant increase in the sensitivity to external inputs, NMDAR hypofunction may affect perception by shifting the dynamic balance between the two modes. Indeed, S-ketamine did not alter the weights of the two-state GLM-HMM (Figure 2C), but increased the probability of external at the expense of internal mode (β = 1.01 ± 0.03, z = 30.7, p = 4.26×10^{-206}, Figure 2D) via an effect on the stay transitions of the HMM (external-to-external and internal-to-internal, Supplemental Figure S3D). This effect was stable over time, and present across the full range of SAR (Figure 2D). Inter-individual differences in the effects of S-ketamine confirmed that NMDAR hypofunction raised the sensitivity to sensory information (Figure 2A) by modulating the time participants spent in external and internal modes, respectively (ρ = 0.41, T(26) = 2.3, p = 0.03). Our results therefore suggest that the failure of sensory attenuation observed under S-ketamine corresponds to an inability to disengage the external mode of perception. Through the lens of predictive processing, the external mode reflects a state of perception that is characterized by an increase in sensory precision at the expense of prior precision. Crucially, it is this balance between sensory and prior precision that determines the Kalman gain. In other words, what matters in terms of perceptual inference are the dynamic changes in relative precision over time.

Strikingly, the data from the Scz-control study mirrored the effect of S-ketamine on the balance between external and internal mode: The two-state GLM-HMM outperformed the standard one-state GLM (patients: $\delta_{BIC} = -981.65$; controls: $\delta_{BIC} = -862.91$) and revealed two opposing modes (Δ_{S-P} = 1.44 ± 0.33, T(44) = 4.33, p = 3.39×10^{-4}, Figure 2F) that alternated in intervals of 265.38 ± 57.76 sec for patients and 230.99 ± 65.04 sec for controls. Patients and controls did not differ with respect to the weights of the two-state GLM-HMM (Figure 2G). Instead, Scz patients spent more time in external mode (β = 0.52 ± 0.03, z = 16.88, p = 1.23×10^{-63}, Figure 2H and Supplemental Figure 4D).

4.3 External and internal modes are perceptual phenomena that cannot be reduced to fluctuations in arousal, fatigue, task engagement, or task difficulty

Our results suggest that healthy participants under S-ketamine and Scz patients spend more time in the external mode. As a dynamic mechanism for psychotic experiences, alternations between external and internal mode should have an effect at the level of perception. This

means that between-mode alternations should modulate a perceptual decision variable that determines not only what is consciously experienced, but also how the contents of perception are evaluated by downstream cognition. The hypothesis that external and internal modes are perceptual phenomena needs to be contrasted against alternative scenarios in which external and internal modes are driven primarily by fluctuations in arousal, high-level cognition, or executive function. This is particularly important, as behavioral reports served as the sole indicators of perceptual states in our paradigm.

To address these alternative accounts, we first performed additional tests to support our claim that external and internal mode operate at the level of perception. External and internal modes are states of a GLM-HMM that integrates the external stimulus s_t with the previous experience y_{t-1} into a perceptual decision variable $P(y_t = 1)$. The parameters of the GLM-HMM are optimized to predict the sequence of perceptual experiences y_t from $P(y_t = 1)$. If external and internal modes are perceptual phenomena, then the stabilization of perception should be driven by the sequence of experiences y_t, as opposed to the sequence of stimuli s_t. To test this hypothesis, we compared our *experienced-based* GLM-HMM, in which the stabilizing internal predictions are driven by the participants' perceptual experience at the preceding overlap, with an alternative *stimulus-based* GLM, in which the stabilizing internal predictions are driven by the stimulus presented at the preceding overlap. Bayesian model comparison indicated that the experienced-based GLM-HMM was better at explaining our data than a stimulus-based GLM-HMM in the S-ketamine experiment ($\delta_{BIC} = -7.4 \times 10^3$) and the case-control study (patients: $\delta_{BIC} = -981.65$; controls: $\delta_{BIC} = -862.91$).

Moreover, if external and internal modes are perceptual phenomena, then the decision variable $P(y_t = 1)$ should not only determine the contents of perception, but also metacognitive processes that depend on them. To assess this prediction, we tested whether the posterior certainty C_t at which the GLM-HMM predicted the content of perception, i.e., the log probability of the experience y_t given the decision variable $P(y_t = 1)$ ($C_t = y_t \cdot \log(P(y_t = 1)) + (1 - y_t) \cdot \log(1 - P(y_t = 1))$), would correlate with the confidence reports c_t in the S-ketamine experiment. This test is a powerful validation of our approach, since the GLM-HMM was only fitted to binary perceptual states y_t, and not to the confidence c_t at which they were reported. Indeed, C_t predicted the confidence reports c_t ($\beta = 0.29 \pm 0.02$, z = 15.4, p = 1.54×10^{-53}) without an interaction with mode ($\beta = -0.07 \pm 0.07$, z = -1.03, p = 0.3), confirming that the positive correlation between posterior certainty and confidence was present in both external and internal modes. C_t extracted from the two-state GLM-HMM was better at explaining confidence than the one-state control GLM (δ_{BIC} = -280.69), and the one-state stimulus GLM (δ_{BIC} = -445.13).

As a consequence, internal mode should be associated with lower metacognitive performance (i.e., the degree to which confidence correlates accuracy), since stabilizing internal predictions have a larger effect on perception in the internal mode, and cause experiences y_t to be less constrained by the external input s_t. Indeed, accuracy was predictive of high confidence ($\beta = 1.01 \pm 0.05$, z = 18.7, p = 4.63×10^{-78}), but to a lesser degree during the internal mode ($\beta = -0.61 \pm 0.09$, z = -6.61, p = 3.94×10^{-11}). In line with this, metacognitive sensitivity, as measured by meta-d', was significantly lower in the internal mode ($\beta = -1.6 \pm 0.45$, T(50) = -3.55, p = 3.41×10^{-3}). Together, these findings support the hypothesis that external and internal modes modulate a low-level decision variable $P(y_t = 1)$ that determines the content of perception and their metacognitive evaluation.

Second, we asked whether fluctuations in global brain states can provide an alternative explanation for external and internal modes. One could assume that mode alternations could in fact reflect dynamic states of arousal, with high arousal and engaged behavior corresponding to the external mode, and low arousal and disengaged behavior corresponding to the internal mode. Our time-resolved assessment of internal states revealed reduced wakefulness (Q1) under S-ketamine (Supplemental Figure S6). This observation is clearly incompatible with the hypothesis that changes in the dynamics of mode are driven by low arousal under S-ketamine, since NMDAR antagonism increased the prevalence of the external mode, improving behavioral performance in the artificial setting of our experiment. When controlling for dynamic changes in wakefulness (Q1), subjective intoxication (Q2) and nervousness (Q3), the effect of S-ketamine on mode (p = 8.21×10^{-67}) and the effect of mode on Δ_{S-P} remained significant (p = 1.29×10^{-5}). We observed no additional effects of or interactions with Q1-3 that could explain the observed relations between S-ketamine, mode, and Δ_{S-P}. Despite its positive effect on perceptual accuracy, external mode was associated with higher levels of dissociation in the S-ketamine experiment as measured by the *Clinician-Administered-Dissociative-States-Scale*[21] (CADSS, $\beta = 1.05 \pm 0.54$, T(208.05) = 1.95, p = 0.05, Supplemental Figure S6B).

In addition to the time-resolved subjective reports on wakefulness obtained under S-ketamine and placebo (Supplemental Figure S6), response times (r_t) can provide an indirect measure of task engagement, with longer r_t and higher r_t variability as indicators of fatigue or disengagement[22,23]. We found no significant effect of mode on r_t in either the S-ketamine experiment ($\beta = 0.02 \pm 0.03$, z = 5.96×10^3, p = 0.78) or in the case-control study ($\beta = 0.03 \pm 0.04$, z = 4.89×10^3, p = 0.76). r_t variability did not differ significantly between modes in the S-ketamine intervention (V = 85, p = 0.47) or in the case-control study (W = 945, p = 0.59). In both experiments, there was no main effect of time on r_t (S-ketamine

intervention: $\beta = 6.11 \times 10^{-3} \pm 0.05$, $T(6.22 \times 10^3) = 0.11$, $p = 1$; case-control study: $\beta = -0.04 \pm 0.05$, $T(5.34 \times 10^3) = -0.71$, $p = 1$). We observed no time-by-intervention interaction ($\beta = 0.04 \pm 0.08$, $T(6.22 \times 10^3) = 0.47$, $p = 1$) nor a time-by-group interaction ($\beta = 0.06 \pm 0.07$, $T(5.35 \times 10^3) = 0.86$, $p = 1$), suggesting that interventions and groups did not differ with respect to fatigue.

Contrary to the natural dynamic of fatigue in psychophysical experiments, which increases over time, we observed no effect of time on the balance between modes in the S-ketamine experiment ($\beta = -0.18 \pm 0.08$, $z = -2.17$, $p = 0.48$, Figure 2D). In the case-control study, external mode even became more prevalent over time ($\beta = 2.41 \pm 0.11$, $z = 21.37$, $p = 4.07 \times 10^{-100}$), with a stronger effect in patients ($\beta = 1.84 \pm 0.14$, $z = 12.97$, $p = 2.83 \times 10^{-37}$, Figure 2H).

Furthermore, we found no evidence that external and internal modes reflect behavioral strategies that depend on task difficulty, such as using internal predictions only when the sensory information is unreliable: Individual stereodisparity thresholds were not correlated with inter-individual differences in mode (Supplemental Figure S6). Within participants, the balance between external and internal mode was only marginally modulated by the SAR of the stimulus (Figure 2D and H).

In sum, these findings suggest that the effect of S-ketamine on mode, and the effects of mode on the integration of external inputs with internal predictions (Δ_{S-P}), are unlikely to be mediated by dynamic changes in arousal, fatigue, task engagement, or task difficulty. Rather, they indicate the NMDAR hypofunction under S-ketamine and in Scz has a direct impact on perceptual processing via its effect on mode.

5 Discussion

Perception integrates incoming signals with internal predictions that reflect prior knowledge about the world[2]. Our results indicate that this integration is subject to dynamic changes over time, alternating between an external mode, where perception closely follows the external input, and an internal mode, where perception is shaped by internal predictions[15,24]. The internal mode enables the brain to use prior knowledge about the statistics of natural environment, such as their temporal autocorrelation, for efficient perception[15]. Intermittent episodes of external mode processing decouple perception from prior knowledge. The balance between external and internal mode may prevent circular inferences within recurrent neural networks, where predictive feedback influences early sensory processing stages[25]. We found

that healthy individuals receiving the NMDAR antagonist S-ketamine, as well as patients diagnosed with Scz, are more prone to an external mode of perception. This NMDAR-dependent change in the balance between modes may expose perception to the destabilizing effects of sensory ambiguity, causing afflicted individuals to be deluded by spurious connections between unrelated events, to attribute the sensory consequences of their actions to an outside force, and to hallucinate signals in noise[1].

5.1 External and internal mode explain dynamic failures of perceptual inference in Scz

During bistable perception, previous experiences provide the predictive context in which incoming sensory data are interpreted, and lead to prolonged periods of perceptual stability despite the ambiguity of the external input[18]. Our results suggest that NMDAR hypofunction, whether due to pharmacological antagonism or as a potential endophenotype of Scz, causes a shift of bistable perception toward the external input, and away from stabilizing internal prediction that stem from previous experiences. These findings bear similarity with prior work on perceptual illusions, where prior knowledge biases perception in ways that may be adaptive in natural environments but reduce perceptual accuracy in experimental settings[26]. Weak predictions may explain why people with Scz are, for example, less susceptible to the hollow-mask illusion, where knowledge about faces is thought to induce the experience of a convex face on the concave surface of a human mask; the Ebbinghaus illusion, where larger circles make a smaller central circle appear bigger; or the force-matching illusion, where humans apply less force when matching an externally applied force with their own[26].

Our findings therefore align with the canonical predictive processing account of psychosis[1]. According to this model, NMDAR hypofunction[7] and Scz[17] are associated with weak priors that cause erratic inferences in perception and cognition, ultimately leading to psychotic symptoms such as delusions and hallucinations. At the same time, they seem at odds with the observation that psychotic experiences, and in particular false alarms that serve as an experimental proxy for hallucinations, correlate with strong priors[27]. So far, attempts to reconcile these disparate sets of findings suggest that priors may vary in strength depending on the phase of psychotic illness, with weak priors in early stages and strong priors in later stages, or depending on their position within the cognitive hierarchy, with weak priors at the perceptual level and strong priors at the cognitive level[1]. As an alternative to predictive processing, circular inference accounts of Scz posit that psychotic symptoms depend on an

over-counting of sensory data that are reverberated multiple times due to an imbalance of excitation and inhibition in feedforward-feedback loops of the cortical hierarchy[28].

In line with the general principles of predictive processing, the GLM-HMM proposed here predicts the experiences y_t in a weighted integration the external input $\beta_S \times s_t$ with internal predictions that embody the temporal autocorrelation of natural environments and are defined by the preceding experiences $\beta_p \times y_{t-1}$. The critical advance provided by the GLM-HMM is that the model allows for dynamic changes in the balance between external and internal sources of information ($\Delta_{S-P} = \beta_S - \beta_P$). In the data presented here, the GLM-HMM revealed that the general shift of perception toward the external input and away from internal predictions observed under S-ketamine and in Scz is in fact driven by changes in the balance between two opposing modes of inference: an external mode, during which priors are weak, and an internal mode, during which priors are strong. The failures of perceptual inference, which are hypothesized to characterize Scz[1], may thus be transient and recurring.

To our knowledge, our results are the first to uncover a neural mechanism underlying the slow, task-related fluctuations in perceptual inference observed in both humans and mice[14,15]. In the context of Scz, this extends previous predictive processing accounts by suggesting an alternative explanation for the apparent discrepancy between strong and weak priors: an imbalance between the modes may cause the brain to make erratic inferences during the external mode, when the influence of previously learned priors is weak, generating a distorted or inaccurate model of the world, which is then used maladaptively during the internal mode, when priors are strong[24]. Furthermore, the dynamic nature of between-mode transitions illustrates how constant and potentially heritable dysfunctions of the NMDAR may produce symptoms of psychosis that are recurrent and transient in nature.

5.2 How are external and internal modes linked to trait-like alterations in Scz and to psychosis-related states of perceptual inference?

In the present data, we did not find a correlation of the balance between external and internal mode with either global psychosis proneness or the clinical severity of Scz (Supplemental Figure S6). Our study was optimized for within-participant power and not designed to detect correlations between inter-individual differences in Scz-related traits and the balance between external and internal modes. One key question moving forward is whether the shift toward external mode represents a general trait-like phenomenon in Scz, potentially linked to cognitive alterations that are also present to some degree under ketamine[29], or whether

external and internal modes are associated with psychosis-related, state-dependent changes in inference.

Future research could address these questions by correlating the balance between modes with both positive and negative symptoms, as well as with measures of cognitive performance such as IQ in larger samples. Another promising approach to distinguish between trait and state effects, which can manifest differently or even with opposite phenotypes[30], could involve real-time symptom tracking combined with functional imaging. Such analyses could help to examine whether shifts between external and internal modes align with the on- and offset of individual psychotic experiences[24], both at the behavioral level and in terms of their neural correlates.

5.3 Are external and internal mode perceptual or behavioral phenomena?

Previous studies have used GLM-HMMs to identify engaged and disengaged behavior in mice tasked with discriminating the location of a visual stimulus[14]. While this terminology may suggest that GLM-HMM states reflect dynamic changes in rodent behavior, evidence from human psychophysics indicates that external and internal modes may in fact reflect perceptual (as opposed to behavioral) states[15,24]. Specifically, when humans detect gratings in white noise, false alarms are more likely when the noise contains more power at the orientation and spatial frequency of the preceding grating, suggesting that detection relies on a predictive perceptual template[19,24]. If these detection events were purely behavioral, no correlation between false alarms and the noise power spectrum would be expected[24]. Critically, recent work demonstrates that these predictive perceptual templates are confined to the internal mode, supporting the hypothesis that the internal mode is indeed predictive and perceptual[24]. Moreover, an analysis of 66 experiments on human two-alternative forced-choice decision-making revealed a quadratic relationship of confidence with mode[15]. The observation that confidence remains high for strong biases toward both external and internal modes[15] argues against the interpretation of internal mode as disengaged behavior.

These observations do not, however, rule out the possibility that external and internal modes have multiple and potentially independent effects on the brain, including influences on high-level cognition and response behavior, or that they are, to some degree, dependent on global brain states. Since our analyses rely on behavioral reports about changes in the content of perception, dynamic changes in response behavior represent an additional potential confound in the identification of external and internal modes. Future work should use trial-wise reports

of perception and confidence with randomized response mappings to enable GLMs that can disentangle perception and response behavior. No-report functional imaging experiments, where the content of experiences is decoded without overt behavioral signals, alongside pupillometry, manipulations of neuromodulators that regulate global brain states, or non-invasive brain stimulation, could help illuminate the causes and consequences of these modes across the cortical hierarchy. Mapping the neurocomputational dynamics of mode alternations will be crucial to testing whether adjusting the balance between modes can mitigate psychotic experiences and ultimately improve the lives of people living with Scz.

6 Data availability

6.1 Lead contact

Further information and requests for resources should be directed to and will be fulfilled by the lead contact, Veith Weilnhammer (veith.weilnhamer@gmail.de).

6.2 Materials availability

This study did not generate new unique reagents.

6.3 Data and code

All data and code associated with this study will be made available on the associated Github repository https://github.com/veithweilnhammer/modes_ketamine_scz upon publication. Key resources are listed in Supplemental Table S1.

7 Acknowledgements

This work was funded by the Leopoldina Academy of Sciences (grant number: LDPS2022-16, https://www.leopoldina.org/en/leopoldina-home/), the German Research Foundation DFG (grant number: STE 1430/9-1, https://www.dfg.de), the Berlin Institute of Health Clinician Scientist Program (https://www.bihealth.org/en/translation/innovation-enabler/academy/bih-charite-clinician-scientist-program), and the German Ministry for Research and Education (ERA-NET NEURON program, grant number: 01EW2007A, https://www.

neuron-eranet.eu/). The funders had no role in study design, data collection, data analysis, decision to publish, or preparation of the manuscript.

8 Competing Interests

The authors report no competing interests.

9 Figures

9.1 Figure 1

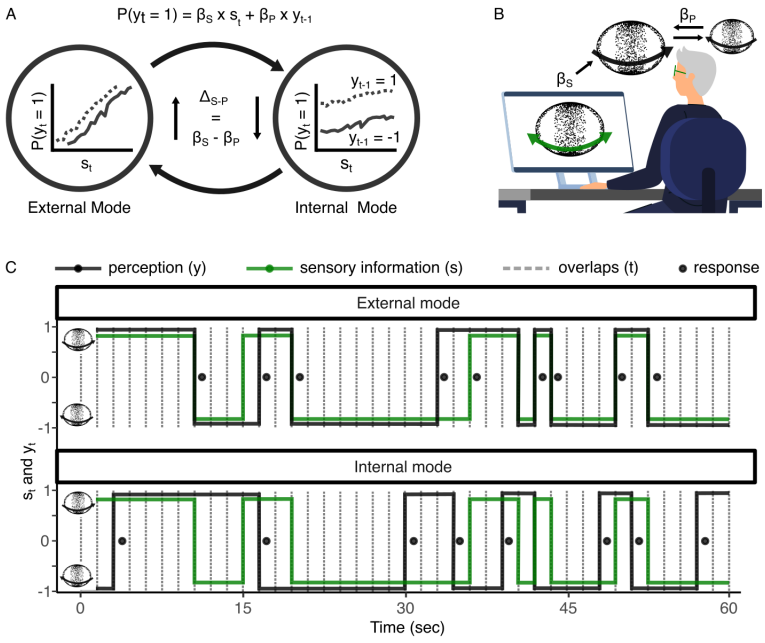

Figure 1.

A. Perception integrates ambiguous sensory signals s_t with internal predictions that reflect prior knowledge about the world. One source of prior knowledge is the temporal autocorrelation of natural environments, where the recent past often predicts the near future. The integration of external inputs and internal predictions depends on the weights assigned to incoming sensory data ($\beta_S \times s_t$) and to internal prediction derived from previous experiences ($\beta_P \times y_{t-1}$, dotted versus solid lines, simulated data), respectively. β_S determines the slope, and β_P the shift of the psychometric function that links s_t and y_t. Importantly, the balance $\Delta_{S-P} = \beta_S - \beta_P$ is known to alternate between two opposing modes: During the external mode (left), perception is largely determined by $\beta_S \times s_t$, which is reflected by a steep slope and a small shift of the psychometric curve. Conversely, during the internal mode (right), perception is shaped by $\beta_P \times y_{t-1}$, resulting in a shallow slope and a large shift of the psychometric curve.

B. We conducted a double-blind placebo-controlled experiment in 28 healthy human participants, who received a continuous infusion with either the NMDAR antagonist S-ketamine or saline. During the infusion, the participants viewed SFM stimuli at varying levels of signal-to-ambiguity (SAR). The stimuli were compatible with two mutually exclusive subjective

experiences (left vs. rightward rotation of the front surface, green arrows). Fully ambiguous stimuli (SAR = 0) induce the phenomenon of bistable perception, where participants perceive spontaneous changes between the two possible interpretations of the stimulus (black arrows) at a rate that is governed by β_P, the degree to which perception is shaped by internal predictions derived from previous experiences. For partially ambiguous stimuli (SAR > 0), perception reflects the weighted integration of internal predictions with external sensory data, which is governed by the balance $\Delta_{S-P} = \beta_S$ - β_P.

C. Changes in the perceived direction of rotation of the SFM stimulus occur at brief depth-symmetric configurations of the stimulus (overlaps, grey dotted lines; Supplemental Video S1). We transformed the behavioral responses into a sequence of states t (1.5 sec intervals, corresponding to the interval between consecutive overlaps), each associated with a combination of the SAR-weighted input s_t (green line) and the perceived direction of rotation y_t (black line). Participants reported whenever they experienced a change in conscious experience (black dots). The response times r_t was defined as the lag between the response and the last preceding overlap. We used HMM-GLMs to quantify the weights β_S, β_P and β_B, which reflect how the reported percepts y_t were determined by the external inputs $\beta_S \times s_t$, the internal predictions $\beta_P \times y_{t-1}$, and the constant bias $\beta_B \times 1$, separately for the external mode (upper panel, 60 sec of example data) and the internal mode (lower panel, 60 sec of example data with identical $s(t)$ for visualization). In the external mode, perception follows the external stimulus closely (high $\Delta_{S-P} = \beta_S - \beta_P$). In the internal mode, perception is shaped more strongly by internal predictions derived from previous experiences (low Δ_{S-P} = β_S - β_P).

9.2 Figure 2

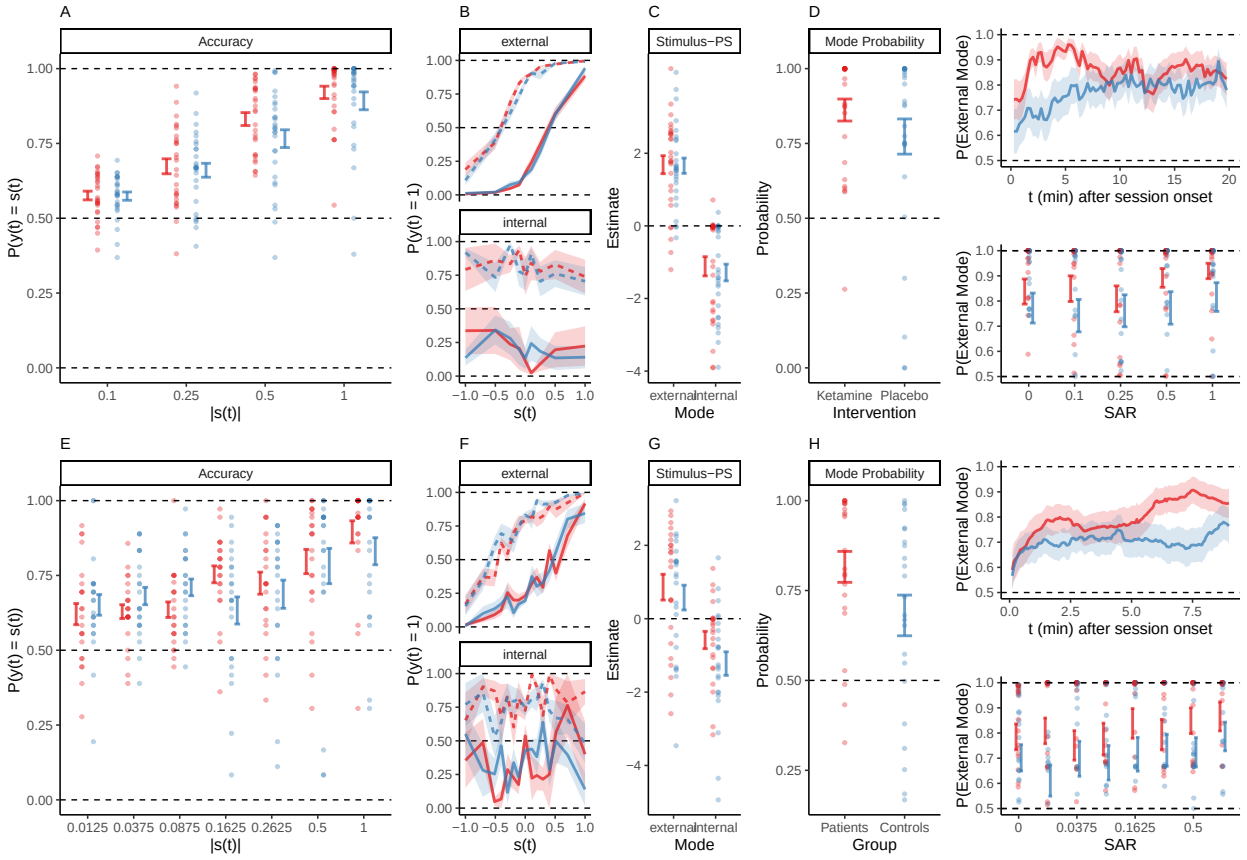

Figure 2.

A. The percepts y_t were more likely to match the stimuli s_t at higher levels of SAR ($\beta = 3.01 \pm 0.06$, z = 50.39, p = 0). The positive effect of SAR on $P(y_t \cong s_t)$ was more pronounced under S-ketamine (red) relative to placebo (blue; $\beta = 0.45 \pm 0.08$, z = 5.6, p = 1.71×10^{-7}).

B. In the S-ketamine experiment, the HMM identified two modes that differed with respect to the relative weighting of external sensory data and internal predictions: Perception fluctuated between an external mode, determined by the input s_t (upper panel panel, steep slope and small shift of the psychometric curve), and an internal mode, dominated by a stabilizing prediction that biased perception toward previous experiences y_{t-1} (lower panel, shallow slope and large shift of the psychometric curve). Within modes, there was no significant effect of S-ketamine (red) versus placebo (blue) on the relation of $y(t)$ with $s(t)$ and $y(t-1)$.

C. Δ_{S-P}, the balance between the external input and the stabilizing internal predictions, was larger during external than during internal mode ($\beta = 2.8 \pm 0.29$, T(−81) = −9.5, p = 5.22×10^{-13}). Importantly, we found no significant effect of S-ketamine (red) vs. placebo (blue) on Δ_{S-P} within modes ($\beta = -0.03 \pm 0.29$, T(81) = −0.1, p = 1).

D. S-ketamine (red) increased the probability of external mode ($\beta = 1.01 \pm 0.03$, z = 30.7, $p = 4.26 \times 10^{-206}$) relative to placebo (blue). The effect of S-ketamine on mode was present from the start of the session ($\beta = 1.77 \pm 0.07$, z = 26.9, $p = 3.55 \times 10^{-158}$, upper right panel), with no significant effect of time ($\beta = -0.18 \pm 0.08$, z = −2.17, p = 0.48). Relative to placebo, S-ketamine increased the probability of external mode across all SARs ($\beta = 0.85 \pm 0.06$, z = 14.14, $p = 3.33 \times 10^{-44}$, lower right panel). Higher SARs were associated with an increased probability of external mode ($\beta = 1.34 \pm 0.09$, z = 15.01, $p = 9.97 \times 10^{-50}$), in particular under S-ketamine ($\beta = 0.62 \pm 0.11$, z = 5.52, $p = 5.27 \times 10^{-7}$). Alternations between external and internal mode were found at all SARs: From from full ambiguity to complete disambiguation, the probability of external mode increased by only 0.11 under S-ketamine and 0.07 under placebo.

E. In patients (red) and controls (blue), percepts y_t were more likely to match the stimuli s_t at higher levels of SAR ($\beta = 2.77 \pm 0.11$, z = 24.85, $p = 2.18 \times 10^{-135}$). Patients followed the external inputs more closely than controls ($\beta = 0.75 \pm 0.15$, z = 4.96, $p = 5.6 \times 10^{-6}$).

F. In analogy to the S-ketamine experiment, the HMM identified two opposing modes in Scz patients (red) and controls (blue). The external mode increased the sensitivity toward s_t (slope of the psychometric function) and weakened the effect of the stabilizing internal prediction y_{t-1} (shift between the dotted and solid line) relative to the internal mode. Within modes, there was no effect of group on the relation of $y(t)$ with $s(t)$ and $y(t-1)$.

G. The external mode increased Δ_{S-P}, the balance between external inputs and internal predictions, in patients (red) and controls (blue; $\beta = 1.44 \pm 0.33$, T(44) = 4.33, $p = 3.39 \times 10^{-4}$), with no significant effect of group ($\beta = -0.28 \pm 0.54$, T(87.97) = −0.52, p = 1).

H. Relative to controls (blue), patients (red) spent more time in external mode ($\beta = 0.52 \pm 0.03$, z = 16.88, $p = 1.23 \times 10^{-63}$). In both group, biases toward external mode increased over time after session onset ($\beta = 2.41 \pm 0.11$, z = 21.37, $p = 4.07 \times 10^{-100}$; upper right panel), with a stronger effect in patients ($\beta = -1.84 \pm 0.14$, z = −12.97, $p = 2.83 \times 10^{-37}$). Patients were more likely than controls to be in external mode across all levels of SAR ($\beta = 0.51 \pm 0.03$, z = 14.56, $p = 7.57 \times 10^{-47}$, lower right panel). External mode increased with SAR ($\beta = 0.63 \pm 0.1$, z = 6.47, $p = 1.54 \times 10^{-9}$), with no significant difference between groups ($\beta = 0.15 \pm 0.13$, z = 1.16, p = 1). As in the S-ketamine experiment, alternations between external and internal mode were found at all SARs: From from full ambiguity to complete disambiguation, the probability of external mode increased by only 0.12 in patients and 0.18 in controls.

10 Supplemental Methods and Figures

10.1 S-ketamine vs. placebo

The S-ketamine experiment consisted in a total of three experimental sessions. During the first session, we screened participants for S-ketamine contraindications (arterial hypertension, prior psychiatric or neurological diagnoses including substance use disorder, use of psychoactive medication), and assessed psychosis proneness using the 40-item *Peters Delusion Inventory* (PDI[31]) and the 32-item *Cardiff Anomalous Perception Scale* (CAPS[32]). Moreover, we conducted three experimental pre-test runs that tested the ability to process stereodisparity (run 1, SAR = 1, cut-off: perceptual accuracy > 0.75), ensured the experience of spontaneous switches during bistable perception (run 2, SAR = 0, cut-off: perceptual stability < 0.96, corresponding to phase durations < 40 sec), and familiarized participants with the main experiment (run 3, see below for details).

In the subsequent two sessions, participants received a continuous intravenous infusion of either S-ketamine at 0.1 mg/kg/h or a saline placebo. Health screenings were repeated before each session to ensure the participants remained eligible. At each day of testing, we checked for alcohol intoxication using a breathalyzer and for recent illicit substance use via a urine drug screen.

Our experimental protocol was double-blinded: The order of S-ketamine and placebo administration was counter-balanced across participants, with at least a two week interval between sessions. The participants, as well as the experimenters tasked with collecting the behavioral and psychometric data, were unaware of whether S-ketamine or placebo was administered by an independent group of clinicians who excluded undiagnosed psychotic illness using the *Brief Psychiatric Rating Scale* (BPRS[33]), established the intravenous line, started the infusion 15 min prior to the experiment, monitored the participants for side effects (blood pressure, drowsiness, vasovagal reactions, and psychotomimetic effects), and removed the intravenous line at the end of the experiment, after which participants were monitored for at least 30 min. Deblinding occurred after data collection was complete.

10.1.1 Sample characteristics

We screened a total of 87 right-handed individuals with (corrected-to-) normal vision, who were naive to the purpose of the study and gave written informed consent before participating. All experimental procedures were approved by the ethics committee at Charité

Berlin.

From the group of screened participants, 31 did not meet our pretest criteria (6 due to perceptual accuracy < 0.75, 15 due to perceptual stability > 0.96, 8 due to substance use, 1 due to do a diagnosis of ADHD, and 1 due to medication with sertraline). Out of the remaining 56 participants who were eligible for the S-ketamine experiment, we aborted the main experiment in 1 participant due to high blood pressure at baseline (RR $>$ 140/80 mmHG), in 2 participants due to strong psychotomimetic effects (micropsia) or dizziness under S-ketamine, and in 1 participant due to a vasovagal syncope during intravenous insertion. 24 participants were not available for the main experiment after successful pre-testing. We therefore report the data from a total of 28 participants (mean age: 28.93 $\pm$ 1.35 years, 18 female) who met all inclusion criteria and completed all experimental sessions.

10.1.2 Experimental paradigm

We presented the experiment using Psychtoolbox 3[34] running in Matlab R2021b (session 1: CRT-monitor at 85 Hz, 1280 x 1024 pixels, 60 cm viewing distance and 39.12 pixels per degree visual angle; session 2 and 32: CRT-monitor at 85Hz, 1280 x 1024 pixels, 40 cm viewing distance and 26.95 pixels per degree visual angle).

Procedure: Throughout the experiment, participants reported their perception of a structure-from-motion (SFM) stimulus (Supplemental Video S1). In this stimulus, random dots distributed on two intersecting rings induce the perception of a spherical object (diameter: 15.86°, rotational speed: 12 sec per rotation, rotations per block: 10, individual dot size: 0.12°) that rotates around a vertical axis with the front surface to the left or right[18]. Stimuli were presented in 120 sec blocks, separated by 10 sec fixation intervals. Please note that we assessed the participants' perception of the stimulus based on a fixed response mapping. In our paradigm, perception and reports are therefore inherently intertwined, with the participants' reports serving as the sole indicators of their perceptual states.

Participants viewed the stimuli through a custom mirror stereoscope. In the pretest experiment, we presented stimuli at complete disambiguation (run 1, SAR = 1), full ambiguity (run 2, SAR = 0) and across five levels ranging from full ambiguity to complete disambiguation across five levels (run 3-5, SAR = [0, 0.1, 0.25, 0.5, 1]). The signal-to-ambiguity ratio (SAR), which was constant within blocks, defines the fraction of stimulus dots that carried a disambiguating 3D signal.

Participants were naive to the potential ambiguity in the visual display, passively experienced the stimulus and reported changes in their perception alongside their confidence via button-

presses on a standard USB keyboard (right middle-finger on k: rotation of the front-surface to the right at high confidence; right index-finger on j: rotation of the front-surface to the right at low confidence; left middle-finger on s: rotation of the front-surface to the left at high confidence; left index-finger on d: rotation of the front-surface to the left at low confidence; thumb on space bar: unclear direction of rotation). Unclear perceptual states occurred at a rate of 0.03 ± 0.01 and were excluded from further analyses.

The direction of rotation enforced by s_t (i.e., whether the parametric 3D signal enforced leftward or rightward rotation of the front surface) changed at a rate of 0.15 per overlap (i.e., on average every 10 sec). Changes in s_t and the order of blocks, each corresponding to one level of SAR, were pseudo-random.

In session 1 (pre-test), each run (runs 1 to 3) consisted of six blocks. In session 2 and 3 (main experiment), each run (run 4 and 5) consisted of 10 blocks. After every third block, the main experiment was paused to allow for the monitoring of the participants' vital signs (blood pressure and pulse rate) and dynamic changes in psychotomimetic experiences. The latter was assessed using the 6 item *Clinician-Administered-Dissociative-States-Scale* (CADSS[21]) and three additional questions (Q1: *How awake do you feel?*, Q2: *How intoxicated do you feel?*, Q3: *How nervous do you feel?*) to which participants responded by clicking on a continuous line that encoded responses from *not at all* to *very much*. To measure global psychotomimetic effects of S-ketamine vs. placebo, participants completed the Questionnaire for the *Assessment of Altered States of Consciousness* (5D-ASC[35]) at the end of session 2 and 3. In addition, we collected responses on a debriefing questionnaire, in which we asked participants to describe whether they were able to accurately perceive the two directions of rotation induced by the SFM stimulus, whether they noticed any differences between blocks, whether they would guess that they received S-ketamine or placebo, and whether they had experienced any effects that they would attribute to a psychoactive substance.

Stereodisparity thresholds: At the beginning of the session 2 and 3, we conducted an independent stereo-acuity test to detect a potential effect of S-ketamine on stereodisparity thresholds[17]. We presented 5000 dots (each at 0.15° visual angle) within a square of 11° x 11° around a central fixation cross (0.10°). We added a stereodisparity signal to all dots on a Landolt C, i.e., a circle (1.37° radius, 2.06° width) with a 90° gap located either at the left, top, right or bottom. Stimuli were presented for 1 sec, after which participants reported the location of the gap by pressing the up-, down-, left- or right-arrow key within a 2 sec response interval, followed by 5 sec of fixation before the next trial.

We adjusted the stereodisparity of the Landolt C in a two-up-one-down staircase across 40 trials (initial stereodisparity: 0.0045°, correct response: decrease in the available stere-

odisparity by one step; incorrect response: increase by two steps, initial step-size: 0.001°, reduction to 0.0005° after first reversal). Stereodisparity thresholds were defined by the average stereodisparity present at the last 10 trials of the staircase.

Scores and Questionnaires: Supplementary Table S2 provides an overview of our psychometric data.

10.2 Scz patients vs. healthy controls

To test whether Scz patients show similar changes in perceptual inference as healthy participants who receive the NMDAR-antagonist S-ketamine, we re-analyzed data from a previously published case-control study[17] that compared Scz patients to healthy participants in paradigm analogous to the S-ketamine experiment described above.

10.2.1 Sample characteristics

We report data from 23 patients diagnosed with paranoid Scz (ICD-10: F20.0, 18 male, age = 37.13±2.42) and 23 controls (17 male, age = 33.57±1.74) that were matched for gender, age and handedness[17].

10.2.2 Experimental paradigm

Stimuli were presented using Psychtoolbox 3[34] running in Matlab R2007b (CRT-Monitor at 60 Hz, 1042x768 pixels, 59.50cm viewing distance, 30.28 pixels per degree visual angle).

Main Experiment: Throughout the experiment, participants reported their perception of a SFM stimulus (see Supplemental Video S2) via button-presses on a standard USB keyboard. In contrast to the S-ketamine experiment, the 300 dots (0.05°) that composed the stimulus (2.05°x 2.05°) were not placed on rings, but on a Lissajous band defined by the perpendicular intersection of two sinusoids ($x(p) = sin(A * p)$ and $y(p) = cos(B * p + \delta)$ with A=3, B=6, with δ increasing from 0 to 2π at 0.15 Hz. Overlapping configurations of the stimulus occurred in intervals of 3.33 sec. Participants viewed the stimuli through a mirror stereoscope. Fusion was supported by rectangular fusion-frames and a background of random dot noise (700 dots of 0.05° which moved at a speed of 1.98° per sec and changed their direction at a rate of 1 Hz).

We presented participants with 3 sessions of the main experiment, each consisting of 14 40.08 sec blocks that were separated by 5 sec of fixation and differed with respect to the SAR,

ranging from full ambiguity to complete disambiguation in 8 levels (SAR = [0, 0.01, 0.04, 0.9, 0.16, 0.26, 0.50, 1]). The frequency of changes in the direction of the disambiguating signal corresponded to the frequency of spontaneous changes that participants perceived during full ambiguity[17] (SAR = 0). In contrast to the S-ketamine experiment, participants only reported the perceived direction of rotation y_t (left vs. rightward movement of the front surface), with no additional assessment of confidence.

Stereodisparity thresholds: We measured stereodisparity thresholds in Scz patients and controls using the procedure described above.

Scores and Questionnaires: We used the PDI[31] and the CAPS[32] to measure delusional ideation and perceptual anomalies in Scz patients and controls. Clinical symptom severity was assessed using the *Positive and Negative Syndrome Scale* (PANSS)[36].

10.3 Quantification and statistical procedures

This manuscript was written in RMarkdown. All data and summary statistics can be reviewed by cloning the Github respository https://github.com/veithweilnhammer/modes_ketamine_scz and running the file *modes_ketamine_scz.Rmd*.

The SFM stimuli used in the above studies share an important feature: Even though physically ambiguous at all angles of rotation, spontaneous changes in the perceived direction of rotation are limited to overlapping configurations of the stimuli[17,18] (see also Supplemental Figure S2 and S4). This is because depth-symmetry, which is a prerequisite for changes in subjective experiences during bistable SFM[17,18], is limited to timepoints when the bands that compose the stimuli overlap (Supplemental Video S1 and S2).

We therefore discretized the perceptual timecourse of all experiments into a sequence of overlaps that occur at times t (1.5 sec inter-overlap interval for the S-ketamine intervention, 3.33 sec inter-overlap interval for the case-control study). We characterized each inter-overlap interval the primary independent variable s_t = [-1, 1] × SAR (the SAR-weighted input ranging from maximum information for leftward rotation to maximum information for rightward rotation), and y_{t-1} (the perceptual experience associated with the preceding overlap). As secondary independent variables, we considered block and session index (reflecting the time participants were exposed to the experiment), participant identifiers and, if applicable, treatment or group identifiers. Primary dependent variables were y_t = [0,1] (the experience of either leftward or rightward rotation) and, if applicable, c_t = [0,1] (low vs. high confidence). As secondary dependent variables, we computed perceptual accuracy (the probability of $y_t \cong s_t$) and perceptual stability (the probability of $y_t = y(t-1)$).

From the perspective of predictive processing, perceptual stability is induced by internal predictions that bias perception toward previous experiences[19]. Stabilizing internal predictions are most likely to be adaptive in natural environments, where the recent past predicts the near future (much like successive frames captured by a video camera are temporarily autocorrelated[19]). Our experiment differed from the temporal autocorrelation of natural environments[19] in that random changes in the direction of disambiguation (i.e., whether the external stimulus supports left- or rightward rotation of the sphere) occurred in average intervals of 10 sec. We thereby created a situation in which strong stabilizing internal predictions *reduce* performance[38]. In our experiment, a shift of perception away from internal predictions toward the external sensory data, which has been proposed to occur under S-ketamine and in Scz[1], should therefore manifest as an *increase* in perceptual accuracy.

For SFM stimuli like those used in this study, changes in experience occur at overlapping configurations of the stimulus[17,18,39,40] (i.e., when the bands that compose the stimulus overlap; see Supplemental Video S1-2). Following previous approaches[17,18,40], we defined response times r_t as the time between a button press that indicates a change in the perceived direction of rotation and the time of the preceding overlapping configuration of the stimulus (see Figure 1C).

To assess differences in metacognitive performance, we correlated perceptual confidence with perceptual accuracy. We computed meta-d', a measure of metacognitive sensitivity that indicates how well confidence ratings predict perceptual accuracy[41].

For all variables, we report and display averages as mean ± standard error of the mean (s.e.m).

10.3.1 Conventional statistics

The goal of our conventional statistics was to quantify the effect of NMDAR hypofunction, whether due to pharmacological antagonism with S-ketamine or due to a diagnosis of Scz, on the interpretation of ambiguous sensory information. We performed standard logistic and linear regression by fitting (general) mixed linear effects models using the R-packages lmer, glmer and afex (see Supplemental Table S2). We predicted y_t, c_t, perceptual accuracy and perceptual stability in logistic regression, and r_t in linear regression. We estimated random intercepts defined within participants in the S-ketamine experiment and nested random intercepts for participants within groups in the case-control study. We applied a Bonferroni-correction for the number of main effects and interactions within models. Mixed effects models are reported with the estimate (β without subscript), followed by the T- or

z-statistic for linear and logistic models, respectively. Please note that parameter estimates with subscripts refer exclusively to the GLM-HMM weights (see Computational modeling) associated with the external input (β_S), the constant bias (β_B), and the previous experience (β_P). For non-normally distributed secondary dependent variables, we performed rank-based tests to assess correlations (Spearman) and distribution differences (Wilcoxon).

10.3.2 Computational modeling

Having established the effect of NMDAR hypofunction on the interpretation of ambiguous sensory information, we used computational modeling to arbitrate between two mechanistic explanations on how S-ketamine and Scz may alter perceptual inference.

Hypothesis H1: Unimodal inference. In one scenario, NMDAR hypofunction may induce a global increase in the sensitivity to external inputs relative to stabilizing internal predictions. This unimodal scenario, which corresponds to the canocical predictive processing hypothesis of Scz[1], assumes S-ketamine- or Scz-related changes in the weights $w \equiv \{\beta_S, \beta_P, \beta_B\}$ of a GLM that predicts percepts y_t from the input vector x_t, which consists in the SAR-weighted external input s_t, the stabilizing internal prediction y_{t-1} and a constant bias b:

$$P(y_t = 1|x_t) = \frac{1}{1 + e^{-x_t \times w}}$$

$$x_t \times w = s_t \times \beta_S + y_{t-1} \times \beta_P + b \times \beta_B$$

According to the unimodal hypothesis H1, NMDAR hypofunction increases β_S at the expense of β_P, leading to an increase of $\Delta_{S-P} = \beta_S$ - β_P.

Hypothesis H2: Bimodal inference. In an alternative scenario, NMDAR hypofunction does not change the weights of the GLM directly, but modulates the transition between latent modes[15] or decision-making strategies[14] that differ with respect to the balance between external inputs s_t and the stabilizing internal prediction provided by y_{t-1}. In the bimodal scenario, perceptual inference is characterized by two latent modes z_t (i.e., states in a HMM) that alternate at a probability per overlap that is defined by a 2 x 2 transition matrix A:

$$P(z_t = k|z_{t-1} = j) = A_{kj}$$

Each state z_t is associated by an independent GLM defined by the weights w_k:

$$P(y_t = 1|x_t, z_t) = \frac{1}{1 + e^{-x_t \times w_k}}$$

$$x_t \times w_k = s_t \times \beta_{S,k} + y_{t-1} \times \beta_{P,k} + b \times \beta_{B,k}$$

Hypothesis H2 differs from the unimodal hypothesis H1 in two ways: First, the two-state GLM-HMM is characterized by two (as opposed to one) GLMs that differ with respect to Δ_{S-P}: In the external mode, β_S is increased relative to β_P. Conversely, in the internal mode, β_P is increased relative to β_S. Second, during bimodal inference, NMDAR hypofunction does not alter the weights within the external and internal GLMs, but modulates the transition probability between the two.

Procedure: To contrast hypotheses H1 and H2, we fitted unimodal and bimodal GLM-HMMs using SSM[42] (Supplemental Table S2), compared models via Bayesian Information Criterion (BIC), and assessed the effects of S-ketamine or Scz on the posterior model parameters, i.e., HMM transition probabilities and the mode-dependent GLM weights w_k. Model fitting using SSM is governed by the hyperparameters σ^2 and α. σ^2 denotes the variance of a prior over the GLM weights w_k. Smaller values of σ^2 shrink w_k toward 0, whereas $\sigma = \infty$ leads to flat priors. We set σ^2 to 100 for GLMs that predicted group-level data, and to 1 for GLMs that predicted participant- or session-level data, which were initialized with group-level estimates of w_k. α defines the Dirichlet prior over the transition matrix A and is flat for $\alpha = 1$. We set α to 1 for all group-level and participant-level fits.

For each experiment, computational modeling was carried out in a sequence of 3 steps: In a first step, we fitted a unimodal GLM initialized with noisy weights to the group-level data (i.e., data pooled across participants within an individual experiment) for a total of n = 100 iterations and computed the average posterior weights w_n. In a second step, we fitted the group-level data with the unimodal and the bimodal GLM-HMM initialized by w_n, extracted the posterior parameters w_k, and compared the models using BIC.

In a third step, we fitted the unimodal and the bimodal GLM-HMM to session-level data (S-ketamine experiment) and participant-level data (case-control experiment). Models were initialized by the average weights w_n of the corresponding group-level model. For all bimodal group-, participant- and session-level GLM-HMMs, we defined the latent mode associated with the higher posterior β_S estimate as external. For summary statistics, we extracted the posterior weights w_k (separately for external and internal mode) and the dynamic posterior probability of external mode $z_t = e$.

The GLM-HMM used in this study predicts experiences y_t in a GLM defined by the stimulus s_t, the preceding experience y_{t-1}, and a constant bias b. The HMM component of the model identifies alternations between two states that differ with respect to the weights of any combination of s_t, y_{t-1}, and b. We used the GLM-HMM to test our primary hypothesis that ketamine and Scz alter the balance between two states that differ with respect to $\Delta_{S-P} = \beta_S$ - β_P (high Δ_{S-P} in external mode, low Δ_{S-P} in internal mode: hypothesis H2). However, the GLM-HMM can, in principle, embody dynamic changes in any combination of β_S, β_B, and β_P. Alternative outcomes to external versus internal modes are states that differ with respect to bias (state 1: high β_B; state 2: low β_B; hypothesis H3) and randomness (state 1: high β_S and β_P; state 2: low β_S and β_P: no difference in Δ_{S-P} between modes: hypothesis H4).

Stimulus- versus experienced-based GLM-HMM. In our experiment, stabilizing internal predictions bias perception toward preceding overlaps (t-1), causing conflicts between the direction of rotation that is consciously experienced (y) and the stimuli s presented at the current overlap t. If external and internal modes are perceptual in nature, then the stabilization of perception should be driven by the sequence of perceptual experiences y, as opposed to the sequence of sensory signals s (hypothesis H5). To test this hypothesis, we compared our *experienced-based* GLM-HMM, in which the stabilizing internal predictions are driven by the participants' perceptual experience at the preceding overlap, with an alternative *stimulus-based* GLM, in which the stabilizing internal predictions are driven by the stimulus presented at the preceding overlap.

External validation of the GLM-HMM. The GLM-HMM generates a perceptual decision variable $P(y_t = 1)$ that is defined by a weighted integration of the external stimulus $(\beta_S \times s_t)$, the previous experience $(\beta_P \times y_{t-1})$, and a constant bias $(\beta_P \times 1)$. The weights are obtained by fitting the GLM-HMM to the sequence of experiences y, irrespective of whether the experience y was made at high or low confidence. This allowed us to test whether the predictions of the two-state GLM-HMM would generalize to metacognitive reports on perception. Importantly, the source of confidence differs between the modes: During the external mode, confidence should depend predominantly on the SAR of the stimulus. Conversely, during the internal mode, confidence should be driven more by the congruency of perception with previous experiences, and less by the external input. To validate our model, we tested whether the perceptual decision variable $P(y_t = 1)$ predicted not only the binary contents of experience y_t (which the GLM-HMM was fitted to), but also perceptual confidence c_t (which the GLM-HMM was not fitted to). To do so, we correlated c_t (as reported by the participants) with the posterior certainty C_t (as provided by the GLM-HMM) at each

overlap. The posterior certainty C_t is given by log probability of the actual experience y, given the decision variable $P(y_t = 1)$:

$$C_t = y_t \cdot \log(P(y_t = 1)) + (1 - y_t) \cdot \log(1 - P(y_t = 1))$$

Please note that the interpretation of our results is inherently limited to the hypotheses incorporated in the above GLMs. In our paradigm, behavioral reports at the time of changes in experience served as the only indicators of the perceptual and metacognitive states of the participants. These behavioral reports were collected with a fixed stimulus-response mapping, such that the GLM-based analyses cannot fully separate perception and response behavior.

Recovery of GLM-HMM parameters. To evaluate the robustness of our GLM-HMM model in estimating mode-dependent weights and transition probabilities, we conducted a parameter recovery analysis. The GLM-HMM is characterized by three weights, β_S, β_B, and β_P, that are defined separately for the external and internal modes. We assessed the model's ability to estimate individual mode-dependent weights by fitting the model to simulated data that were obtained by sampling from GLM-HMMs in which individual target weights were systematically varied, while all other weights were kept constant at the group-level average obtained from the original data. For each analysis, we selected one of the six weights (3 weights $\times$ 2 modes) and varied its value parametrically from -1 to 5. We then generated synthetic data, simulating y_{syn} for n = 78400 overlaps (corresponding to the number of overlaps observed across all participants in the S-ketamine experiment). The GLM-HMM model was then fitted to these synthetic data.

We repeated the recovery analysis for each weight 10 times, computed the average posterior weights β_S, β_B, and β_P, and then correlated these recovered weights with the synthetic input weights. We applied a similar procedure to evaluate the recovery of the GLM-HMM transition matrix. Transition probabilities were varied parametrically within the range of 0.8 to 1 for on-diagonal cells (external to external, internal to internal) and 0 to 0.2 for off-diagonal cells (external to internal, internal to external). The results of this recovery analysis, which are depicted in Supplemental Figure S1, demonstrate that the GLM-HMM weights and transition probabilities can be recovered with high fidelity across the full range of the synthetic input parameters, and in particular in the parameter region of the group-level estimates obtained from the original data (w_n).

10.4 Supplemental Figure S1

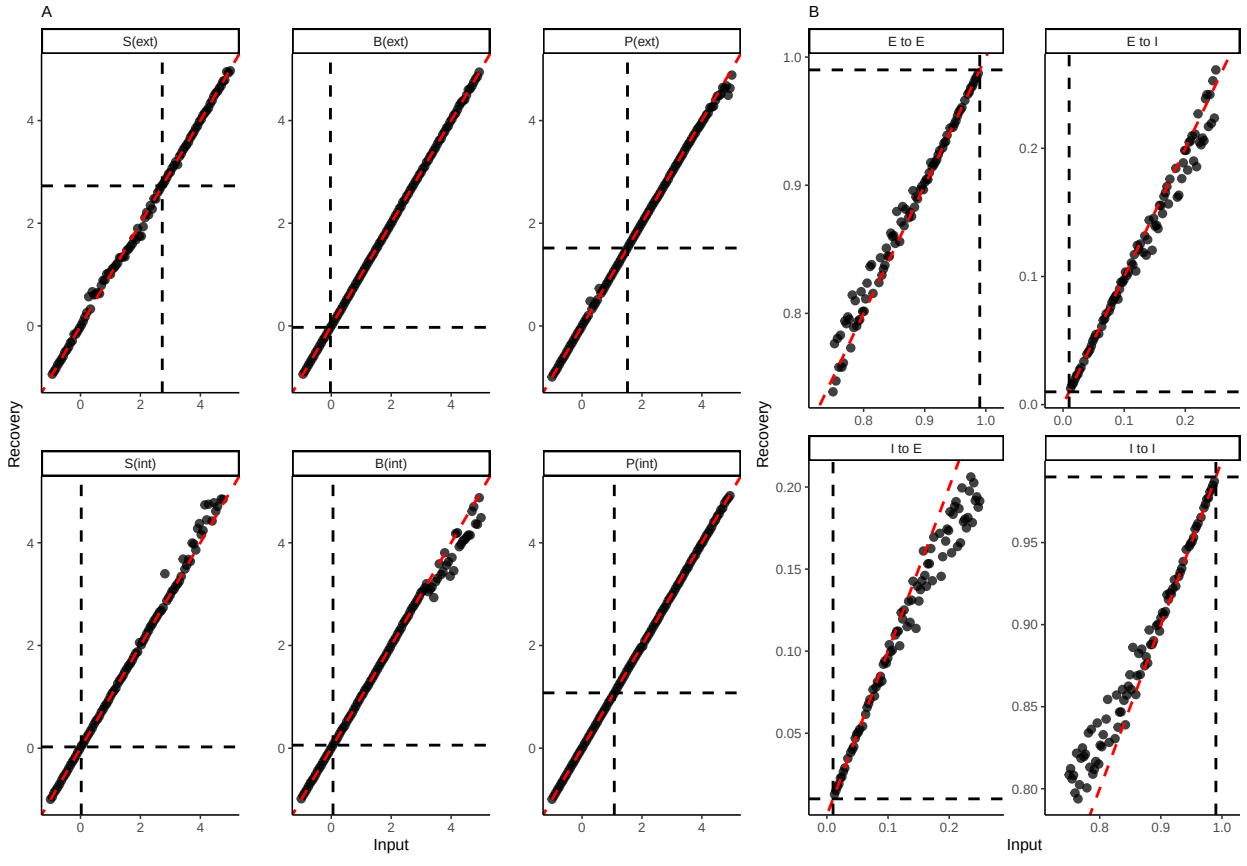

Supplemental Figure S1. GLM-HMM parameter recovery

A. Weight recovery from simulated data: GLM weights. The GLM-HMM is defined by the mode-dependent weights β_S, β_B, and β_P. To test how well our GLM-HMM can recover changes in individual weights, we selected one of the six weights (3 weights x 2 modes) and varied its value parametrically from -1 to 5. For each inversion, we kept all other weights at the group-level average obtained from the original data. For each of the six recovery analyses, we simulated synthetic experiences y_{syn} for n = 78400 overlaps (number of overlaps across participants in the S-ketamine experiment). We then fitted a randomly initialized GLM-HMM to the synthetic experiences, and extracted the weights recovered from the synthetic experiences y_{syn}. We performed each recovery for 10 iterations, computed the average posterior weights β_S, β_B, and β_P, and correlated them with the synthetic input weights. The correlation with the parametric input weights and the posterior weights recovered from the simulated data were close to 1 for all weights (β_S, β_B, and β_P, columns) and modes (external and internal, rows). Weights were recovered with high fidelity across a broad range of weights (average r = 0.99), and in particular at the group-level weights w_n obtained from the original data (black dotted line). The red dashed line represents the

identity line (slope = 1, intercept = 0), indicating perfect recovery.

B. Weight recovery from simulated data: transition matrix. We repeated the above procedure for each cell of the GLM-HMM transition matrix. We initialized models with parametric transition probabilities ranging from 0.8 to 1 (on-diagonal cells, external to external, internal to internal) and 0 to 0.2 (off-diagonal cells, external to internal, internal to external). Transition probabilities were recovered with high fidelity across a broad range of parameters (average r = 0.99), and in particular at the group-level estimates obtained from the original data (black dotted line). The red dashed line represents the identity line (slope = 1, intercept = 0), indicating perfect recovery.

10.5 Supplemental Figure S2

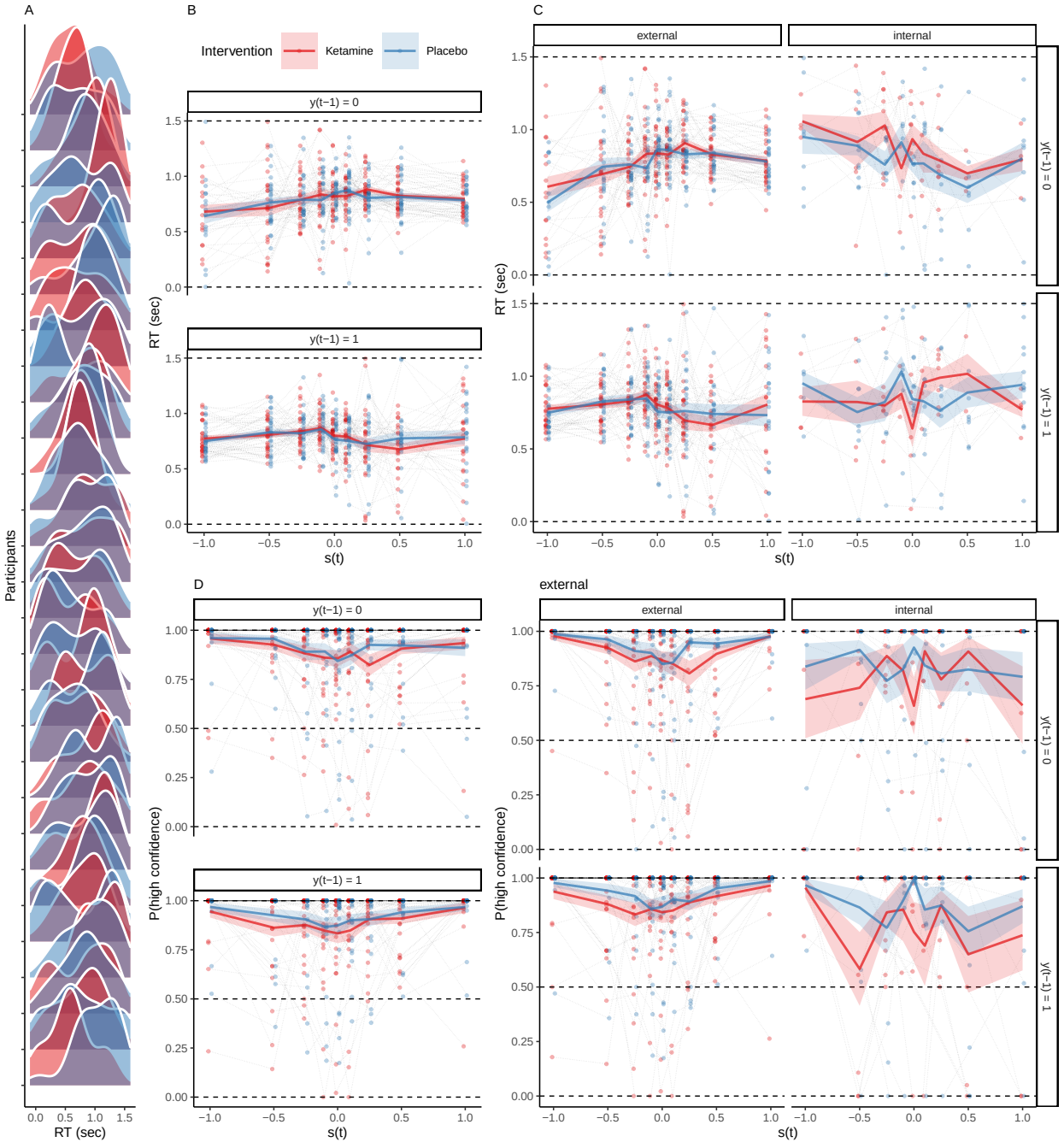

Supplemental Figure S2. The effects of ketamine and bimodal inference on RT.

A. RT were non-uniformly distributed across the inter-overlap interval (D = 0.09, p = 5.38×10^{-9}, one-sample Kolmogorov-Smirnov test). This corroborates that changes in perception aligned with the overlapping configurations of the stimulus after S-ketamine (red) and placebo (blue).

B. RT showed a quadratic relationship with s_t ($\beta = -6.87 \pm 1.68$, $T(6.2 \times 10^3) = -4.1$, $p = 5.1 \times 10^{-4}$), indicating faster responses when sensory information was reliable ($|s_t| \gg 0$; note that SAR as shown in Figure 2A and 2E is equal to $|s_t|$). We observed no main effect of S-ketamine (red) vs. placebo (blue) on RT ($\beta = -3.35 \times 10^{-3} \pm 0.01$, $T(6.2 \times 10^3) = -0.32$, $p = 1$).

C. We found no additional effect of mode on RT ($\beta = 0.02 \pm 0.03$, $z = 5.96 \times 10^3$, $p = 0.78$).

D. Confidence showed a quadratic relationship with s_t ($\beta = 74.83 \pm 2.39$, $z = 31.32$, $p = 3.22 \times 10^{-214}$), confirming that participants were more confident when sensory information was reliable ($|s_t| = SAR \gg 0$). Relative to placebo (blue), S-ketamine (red) reduced choice confidence ($\beta = -0.21 \pm 0.04$, $z = -5.9$, $p = 4.36 \times 10^{-8}$), and decreased the quadratic effect of s_t on confidence ($\beta = -19.95 \pm 2.36$, $z = -8.45$, $p = 3.48 \times 10^{-16}$).

E. External mode increased confidence globally ($\beta = 0.72 \pm 0.07$, $z = 9.92$, $p = 7.85 \times 10^{-22}$) and by elevating the quadratic effect of s_t on confidence ($\beta = 242.61 \pm 18.43$, $z = 13.16$, $p = 3.37 \times 10^{-38}$). When controlling for mode, the negative effect of S-ketamine (red) vs. placebo (blue) on confidence and on the quadratic relationship of confidence with s_t remained significant.

10.6 Supplemental Figure S3

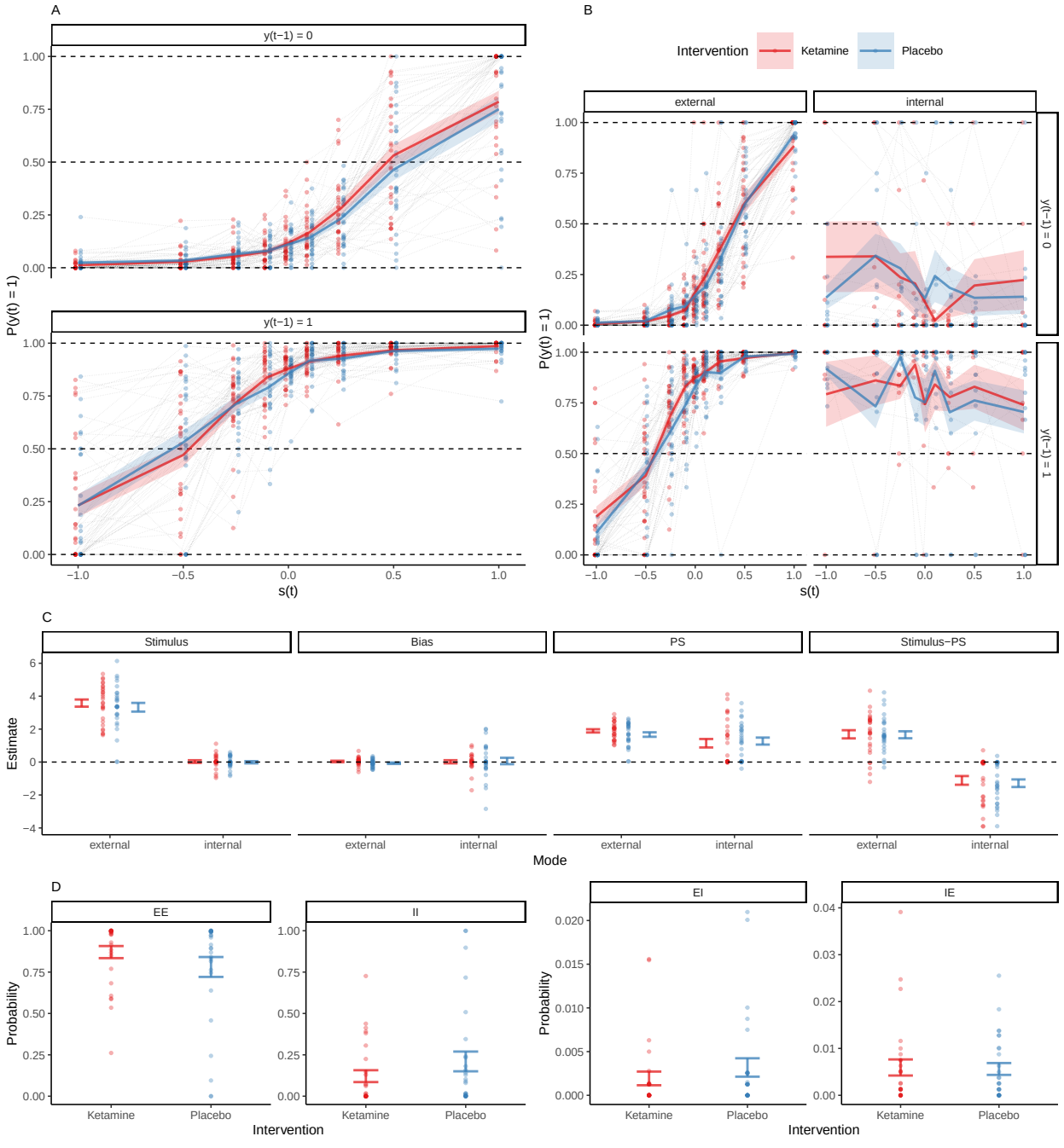

Supplemental Figure S3. Extended data on the effects of S-ketamine and mode on perceptual inference (related to Figure 2A-C).

A. Here, we show psychometric curves (percept y_t versus input s_t) under S-ketamine (red) and placebo (blue). The plot separates times t for which the previous experience was leftward rotation ($y_{t-1} = -1$, upper panel) and rightward rotation ($y_{t-1} = +1$, lower panel). As

expected, y_t was driven by both the external input s_t ($\beta_S = 3.01 \pm 0.06$, z = 50.39, p = 0) and the previous percept y_{t-1} ($\beta_P = 2.06 \pm 0.03$, z = 80.58, p = 0). We found no significant interaction between the s_t and y_{t-1} ($\beta = -0.06 \pm 0.06$, z = -1.06, p = 1). Relative to placebo, S-ketamine caused a shift of y_t toward s_t ($\beta = 0.45 \pm 0.08$, z = 5.6, p = 1.71×10^{-7}), with no significant effect on y_{t-1} ($\beta = 0.08 \pm 0.04$, z = 2.39, p = 0.13). We found no significant three-way-interaction (drug x s_t x y_{t-1}, $\beta = -0.07 \pm 0.08$, z = -0.9, p = 1).

B. This panel shows the data from panel (A) separately for times t where the HMM identified the mode of perceptual inference as external (left panels) or internal (right panels). When the mode of perceptual processing was added to the prediction of y_t from s_t and y_{t-1}, the effect S-ketamine (red) vs. placebo (blue) on s_t disappeared ($\beta = 0.24 \pm 0.11$, z = 2.13, p = 0.53). Instead, changes in the balance between s_t and y_{t-1} were loaded onto fluctuations between external and internal mode, which caused perception to shift away from external inputs s_t ($\beta = -4.23 \pm 0.21$, z = -20.01, p = 7.54×10^{-88}) and toward previous experiences $yt - 1$ ($\beta = 0.78 \pm 0.09$, z = 8.64, p = 8.81×10^{-17}).

C. Here, we plot the weights from the GLM $y_t = \beta_S \times s_t + \beta_P \times y_{t-1} + \beta_B \times 1$, alongside the balance between external inputs and previous experiences $\Delta_{S-P} = \beta_S - \beta_P$ during external and internal mode. Colors indicate S-ketamine (red) and placebo (blue). β_S, the weight associated with the external input s_t, was positive in external mode, but reduced to zero in internal mode ($\beta = -3.55 \pm 0.23$, T(81) = -15.44, p = 4.78×10^{-24}). We found no additional effect of S-ketamine (red) versus placebo (blue; $\beta = -0.25 \pm 0.23$, T(81) = -1.1, p = 1) and no significant interaction ($\beta = 0.21 \pm 0.33$, T(81) = 0.65, p = 1). β_B, the weight associated with the constant response bias b toward rightward rotation, was not different from zero ($\beta_B = 0.04 \pm 0.11$, T(98.36) = 0.31, p = 1). We found no effect of drug ($\beta = -0.11 \pm 0.14$, T(81) = -0.74, p = 1) or mode ($\beta = -0.02 \pm 0.14$, T(81) = -0.12, p = 1) on the bias weight β_B. β_P, the weight associated with the previous percept y_{t-1} was not modulated by S-ketamine ($\beta = -0.22 \pm 0.26$, T(81) = -0.87, p = 1) or mode ($\beta = -0.75 \pm 0.26$, T(81) = -2.92, p = 0.29). There was no significant interaction between drug and mode with respect to β_P ($\beta = 0.35 \pm 0.36$, T(81) = 0.97, p = 1). The balance Δ_{S-P} between external inputs and internal predictions was determined by mode ($\beta = 2.8 \pm 0.29$, T(81) = 9.5, p = 5.22×10^{-13}), with no significant effect of S-ketamine ($\beta = 0.03 \pm 0.29$, T(81) = 0.1, p = 1) and no interaction ($\beta = 0.14 \pm 0.42$, T(81) = 0.34, p = 1). These posterior GLM-HMM weights argue against the alternative hypotheses that the primary effect of S-ketamine is related to changes in dynamics of bias (state 1: high β_B; state 2: low β_B; hypothesis H3) or the randomness of experience (state 1: high β_S and β_P; state 2: low

β_S and β_P with no difference in Δ_{S-P} between modes: hypothesis H4).

D. S-ketamine (red) increased the probability of external mode ($\beta = 1.01 \pm 0.03$, z = 30.7, p = 4.26×10^{-206}) relative to placebo (blue) by elevating the stability of external at the expense of internal mode (EE versus II; left panels; V = 264, p = 0.01), with no effect on the transition probabilities between modes (EI versus IE; right panels; V = 149, p = 0.37).

10.7 Supplemental Figure S4

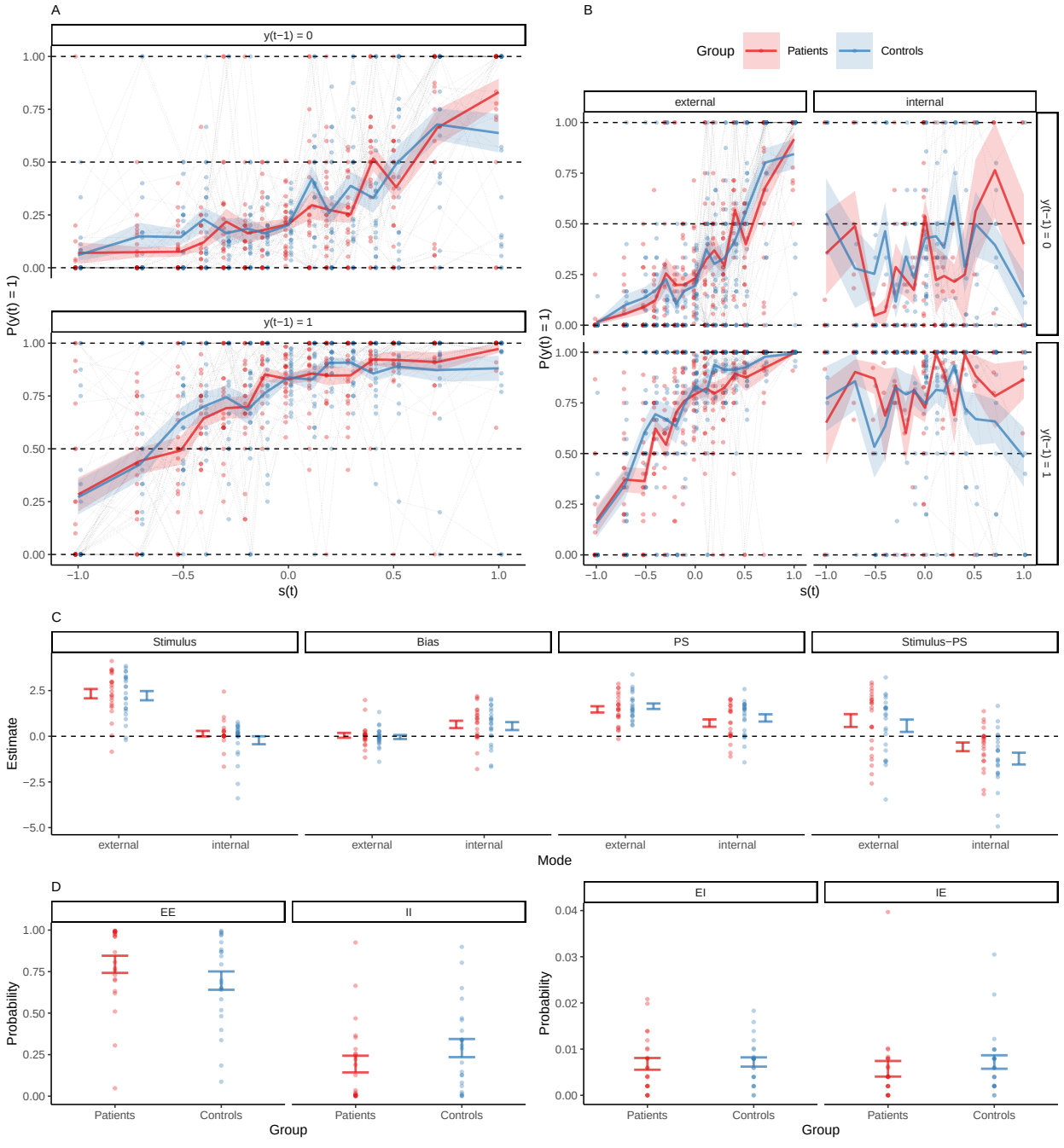

Supplemental Figure S4. Extended data on external and internal mode in Scz patients and healthy controls (related to Figure 2E-H).

A. Here, we show psychometric curves (percept y_t versus input s_t) in patients (red) and controls (blue). The plot separates times t for which the previous experience was leftward rotation ($y_{t-1} = -1$, upper panel) and rightward rotation ($y_{t-1} = +1$, lower panel). Per-

ception was driven by s_t ($\beta_S = 2.77 \pm 0.11$, z = 24.85, p = 2.18×10^{-135}) and y_{t-1} ($\beta_P = 1.5 \pm 0.03$, z = 58.2, p = 0), with no significant interaction between s_t and y_{t-1} ($\beta = -5.41 \times 10^{-3} \pm 0.11$, z = −0.05, p = 1). Patients were more sensitive to s_t ($\beta = 0.75 \pm 0.15$, z = 4.96, p = 5.6×10^{-6}). We found no significant three-way-interaction (group x s_t x y_{t-1}, $\beta = -0.37 \pm 0.15$, z = −2.45, p = 0.11).

B. This panel shows the data from panel (A) separately for times t where the HMM identified the mode of perceptual inference as external (left panels) or internal (right panels). When the mode of perceptual processing was added to the prediction of y_t from s_t and y_{t-1}, the difference between patients (red) and controls (blue) in the effect of s_t on y_t disappeared ($\beta = -0.02 \pm 0.22$, z = −0.08, p = 1). Instead, changes in the balance between s_t and y_{t-1} were loaded onto fluctuations between external and internal mode, which caused perception to shift away from external inputs s_t ($\beta = -3.47 \pm 0.29$, z = −11.95, p = 1.01×10^{-31}) and toward previous experiences $yt - 1$ ($\beta = 0.5 \pm 0.07$, z = 6.85, p = 1.15×10^{-10}).

C. Here, we plot the weights from the GLM $y_t = \beta_S \times s_t + \beta_P \times y_{t-1} + \beta_B \times 1$, alongside the balance between external inputs and previous experiences $\Delta_{S-P} = \beta_S - \beta_P$ during external and internal mode. Colors indicate the group (patients in red, controls in blue). β_S, the weight associated with the external input s_t, was positive in external mode, but reduced to zero in internal mode ($\beta = -2.19 \pm 0.24$, T(44) = −9.13, p = 4.07×10^{-11}). We found no additional effect of group ($\beta = -0.11 \pm 0.37$, T(87.69) = −0.3, p = 1) and no significant interaction ($\beta = -0.25 \pm 0.34$, T(44) = −0.74, p = 1). β_B, the weight associated with the constant response bias b toward rightward rotation, was not different from zero ($\beta = 0.05 \pm 0.18$, T(1.62×10^{-8}) = 0.29, p = 1). We found no effect of group ($\beta = -0.09 \pm 0.25$, T(1.62×10^{-8}) = −0.37, p = 1). There was a trend for a positive effect of internal mode ($\beta = 0.6 \pm 0.24$, T(88) = 2.47, p = 0.06) on the bias weight β_B. β_P, the weight associated with the previous percept y_{t-1}, was reduced in internal mode ($\beta = -0.75 \pm 0.26$, T(88) = −2.92, p = 0.02), but not modulated by group ($\beta = 0.17 \pm 0.32$, T(9.88×10^{-10}) = 0.54, p = 1). There was no significant interaction between group and mode with respect to β_P ($\beta = 0.11 \pm 0.36$, T(88) = 0.3, p = 1). The balance Δ_{S-P} between external inputs and internal predictions was determined by mode ($\beta = 1.44 \pm 0.33$, T(81) = 9.5, p = 3.39×10^{-4}), with no significant effect of group ($\beta = 0.28 \pm 0.54$, T(87.97) = 0.52, p = 1) and no interaction ($\beta = 0.36 \pm 0.47$, T(44) = 0.76, p = 1). These posterior GLM-HMM weights argue against the alternative hypotheses that the primary effect of S-ketamine is related to changes in dynamics of bias (state 1: high β_B; state 2: low β_B; hypothesis H3) or the randomness of experience (state 1: high β_S and β_P; state 2: low β_S and β_P with no difference in Δ_{S-P} between modes: hypothesis H4).

D. Relative to controls (blue), patients (red) spent more time in external mode ($\beta = 0.52 \pm 0.03$, $z = 16.88$, $p = 1.23 \times 10^{-63}$). This effect was driven by an increase in the stability of external mode at the expense of internal mode (EE versus II; left panels; $W = 352$, $p = 0.03$). There was no effect of group on the transition probabilities between modes (EI versus IE; right panels; $W = 248$, $p = 0.65$).

10.8 Supplemental Figure S5

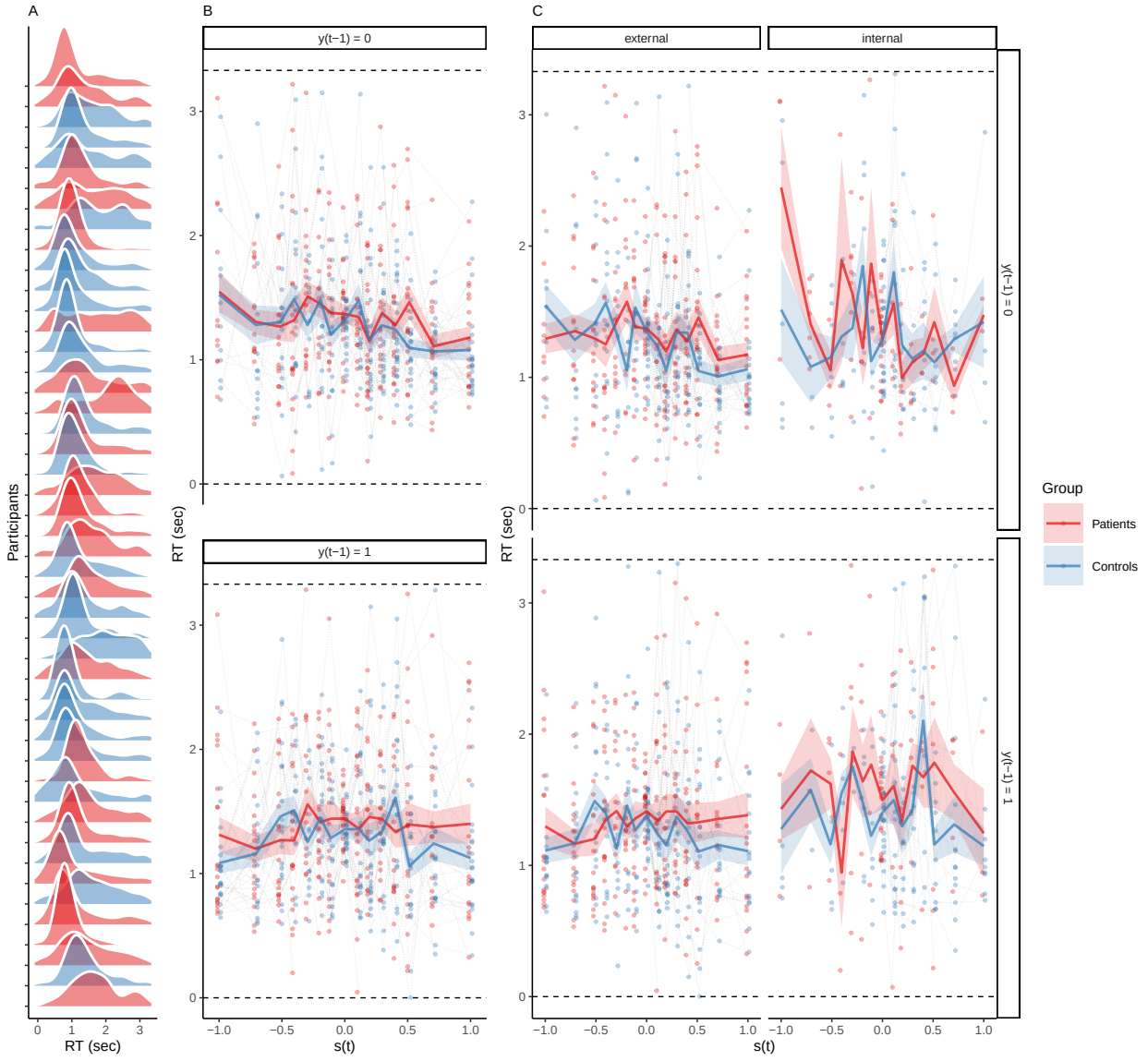

Supplemental Figure S5. RT and bimodal inference in Scz patients and controls.

A. RT were non-uniformly distributed across the inter-overlap interval (D = 0.22, p = 2.39×10^{-232}, one-sample Kolmogorov-Smirnov test against uniformity) in patients (red) and controls (blue). This confirmed that changes in perception were aligned with the overlapping configurations of the stimulus.

B. RT did not differ between patients (red) and controls (blue; $\beta = -0.07 \pm 0.08$, T(66.96) $= -0.87$, p = 1). We found no quadratic relationship between RT and s_t ($\beta = -3.54 \pm 2.34$, T(5.33×10^3) $= -1.51$, p = 1).

C. We found no effect of mode on RT ($\beta = 0.03 \pm 0.04$, z = 4.89×10^3, p = 0.76).

10.9 Supplemental Figure S6

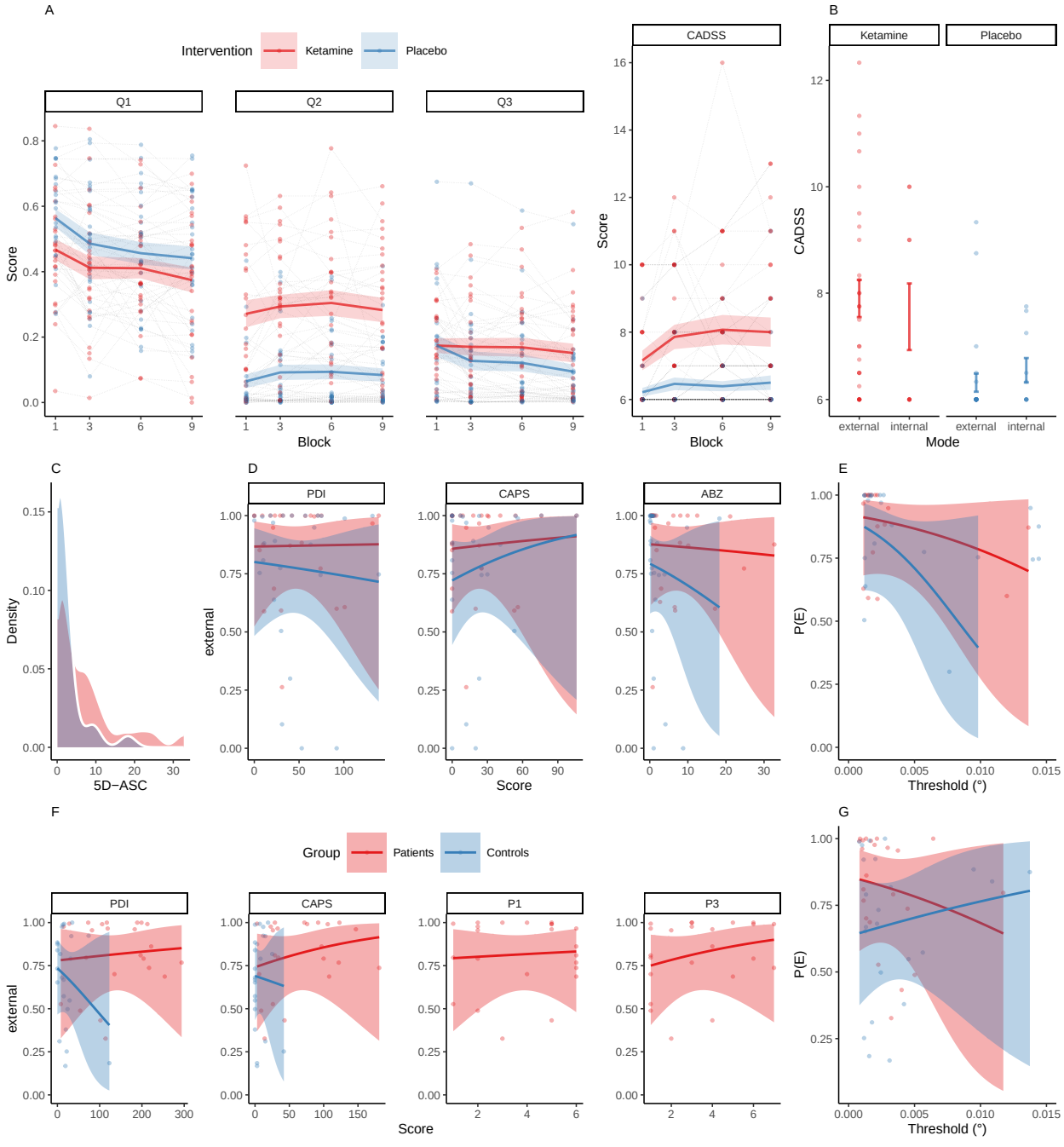

Supplemental Figure S6. Scores and Questionnaires.

A. Responses to Q1 (*How awake do you feel?*) indicated that participants felt more tired under S-ketamine (red) than placebo (blue; $\beta = -1.53 \pm 0.6$, $z = -2.57$, $p = 0.04$), with no significant effect of time or a between-factor interaction. Responses to Q2 (*How intoxicated do you feel?*) indicated that participants felt more intoxicated under S-ketamine ($\beta = 3.32$

$\pm$ 1.44, z = 2.3, p = 0.09), with no significant effect of time or a between-factor interaction. Responses to Q3 (*How nervous do you feel?*) revealed no effect of S-ketamine ($\beta = -3.01 \pm 2.62$, z = −1.15, p = 1), time, nor a significant between-factor interaction. CADSS scores were elevated under S-ketamine ($\beta = 1.01 \pm 0.34$, T(185.32) = 2.99, p = 0.01) with a borderline trend for an increase over time (0.09 ± 0.04, T(185.61) = 2.24, p = 0.1) and no significant between-factor interaction.

B. Q1-3 and CADSS scores were collected after blocks 1, 3, 6 and 9. To assess how the mode of perceptual inference was linked to dissociative symptoms, we separated the participants ratings according to the mode that dominated perception at the very end of the preceding block. While controlling the effect of S-ketamine (red) vs placebo (blue), we found that external mode increased dissociative symptoms ($\beta = 1.05 \pm 0.54$, T(208.05) = 1.95, p = 0.05), but had no effect on wakefulness (Q1), subjective intoxication (Q2) or nervousness (Q3).

C. 5-ASC scores were elevated under S-ketamine (red) relative to placebo (blue; $\beta = 4.89 \pm 1.59$, T(27.14) = 3.08, $p = 9.33 \times 10^{-3}$).

D. Neither PDI, CAPS, nor 5-ASC scores were predictive of the probability of external mode (shown separately for S-ketamine in red and placebo in blue).

E. Stereodisparity thresholds were not predictive of the probability of external mode ($\beta = -28.73 \pm 781.1$, z = −0.04, p = 0.97). Thresholds did not differ between S-ketamine (red) and placebo (blue; W = 102, p = 0.66).

F. Neither PDI, CAPS (patients in red and controls in blue), nor the PANSS items P1 (delusions) or P3 (hallucinations, patients only) predicted the probability of external mode.

G. In patients (red) and controls (blue), stereodisparity thresholds were not predictive of the probability of external mode ($\beta = -1.88 \pm 2.05$, z = −0.92, p = 1). Thresholds did not differ between groups (V = 976, p = 0.52).

10.10 Supplemental Table S1

RESOURCE	SOURCE	IDENTIFIER
Deposited data & code		
Analyzed data & custom code	https://github.com/veithweilnhammer/modes_ketamine_scz/	N/A
Software		
Matlab	https://www.mathworks.com/	RRID:SCR_001622
Psychtoolbox 3	http://psychtoolbox.org/	RRID:SCR_002881
R	http://www.r-project.org/	RRID:SCR_001905
RStudio	https://www.rstudio.com/	RRID:SCR_000432
lme4, afex, statConfR, ggplot2, ggridges, gridExtra, tidyr, plyr, readxl	http://cran.r-project.org/	RRID:SCR_003005
Python 3	http://www.python.org/	RRID:SCR_008394
Jupyter Notebook	https://jupyter.org/	RRID:SCR_018315
numpy	http://www.numpy.org	RRID:SCR_008633
pandas	https://pandas.pydata.org	RRID:SCR_018214
SSM	https://github.com/lindermanlab/ssm	N/A

Supplemental Table S1. Key resources.

10.11 Supplemental Table S2

Scale	Scope	Condition	mean ± s.e.m.
PDI[31]	Delusion proneness	Global	46.22 ± 7.19
CAPS[32]	Hallucination proneness	Global	23 ± 5.05
BPRS[33]	Screen for psychotic illness	Global	0.64 ± 0.27
5D-ASC[35]	Altered states of consciousness	S-ketamine	7.11 ± 1.59
		Placebo	2.2 ± 0.75
CADSS[21]	Dissociation	S-ketamine	7.8 ± 0.33
		Placebo	6.43 ± 0.17
Q1	Wakefulness	S-ketamine	0.41 ± 0.03
		Placebo	0.48 ± 0.03
Q2	Intoxication	S-ketamine	0.29 ± 0.03
		Placebo	0.09 ± 0.02
Q3	Nervousness	S-ketamine	0.17 ± 0.02
		Placebo	0.13 ± 0.03
Stereovision	Disparity thresholds	S-ketamine	$2.89 \times 10^{-3} \pm 6.18 \times 10^{-4}$
		Placebo	$2.75 \times 10^{-3} \pm 4.39 \times 10^{-4}$

Supplemental Table S2. Psychometric data for the S-ketamine experiment.

10.12 Supplemental Table S3

Scale	Scope	Condition	mean ± s.e.m.
PDI[31]	Delusion proneness	Patients	138.83 ± 16.64
		Controls	21.87 ± 5.75
CAPS[32]	Hallucination proneness	Patients	65.17 ± 10.56
		Controls	7.13 ± 2.2
P1	Delusions	Patients	3.83 ± 0.39
P3	Delusions	Patients	3.35 ± 0.44
Stereovision	Disparity thresholds	Patients	$2.82 \times 10^{-3} \pm 5.13 \times 10^{-4}$
		Controls	$3.46 \times 10^{-3} \pm 7.14 \times 10^{-4}$

Supplemental Table S3. Psychometric data for Scz-control-study.

References

1. Sterzer, P. *et al.* The Predictive Coding Account of Psychosis. *Biological Psychiatry* **84**, 634–643 (2018).
2. Friston, K. A theory of cortical responses. *Philosophical transactions of the Royal Society of London. Series B, Biological sciences* **360**, 815–836 (2005).
3. Rao, R. P. *et al.* Predictive coding in the visual cortex: A functional interpretation of some extra-classical receptive-field effects. *Nature neuroscience* **2**, 79–87 (1999).
4. Feldman, H. *et al.* Attention, uncertainty, and free-energy. *Frontiers in Human Neuroscience* **4**, 7028 (2010).
5. Muthukumaraswamy, S. D. *et al.* Evidence that Subanesthetic Doses of Ketamine Cause Sustained Disruptions of NMDA and AMPA-Mediated Frontoparietal Connectivity in Humans. *Journal of Neuroscience* **35**, 11694–11706 (2015).
6. Corlett, P. R. *et al.* Glutamatergic Model Psychoses: Prediction Error, Learning, and Inference. *Neuropsychopharmacology* **36**, 294–315 (2011).
7. Stein, H. *et al.* Reduced serial dependence suggests deficits in synaptic potentiation in anti-NMDAR encephalitis and schizophrenia. *Nature Communications* **11**, 1–11 (2020).
8. Murray, J. D. *et al.* Linking Microcircuit Dysfunction to Cognitive Impairment: Effects of Disinhibition Associated with Schizophrenia in a Cortical Working Memory Model. *Cerebral Cortex* **24**, 859–872 (2014).
9. Catts, V. S. *et al.* A quantitative review of the postmortem evidence for decreased cortical N-methyl-D-aspartate receptor expression levels in schizophrenia: How can we link molecular abnormalities to mismatch negativity deficits? *Biological Psychology* **116**, 57–67 (2016).
10. Adams, R. A. *et al.* Computational Modeling of Electroencephalography and Functional Magnetic Resonance Imaging Paradigms Indicates a Consistent Loss of Pyramidal Cell Synaptic Gain in Schizophrenia. *Biological Psychiatry* **91**, 202–215 (2022).
11. Self, M. W. *et al.* Different glutamate receptors convey feedforward and recurrent processing in macaque V1. *Proceedings of the National Academy of Sciences* **109**, 11031–11036 (2012).
12. Castro-Alamancos, M. A. *et al.* Short-term synaptic enhancement and long-term potentiation in neocortex. *Proceedings of the National Academy of Sciences* **93**, 1335–1339 (1996).

1039 13. Nakazawa, K. *et al.* Spatial and temporal boundaries of NMDA receptor hypofunction leading to schizophrenia. *npj Schizophrenia* **3**, 1–11 (2017).

1040 14. Ashwood, Z. C. *et al.* Mice alternate between discrete strategies during perceptual decision-making. *Nature Neuroscience* **25**, 201–212 (2022).

1041 15. Weilnhammer, V. *et al.* Sensory processing in humans and mice fluctuates between external and internal modes. *PLOS Biology* **21**, e3002410 (2023).

1042 16. Albert, S. *et al.* A hierarchical stochastic model for bistable perception. *PLOS Computational Biology* **13**, e1005856 (2017).

1043 17. Weilnhammer, V. *et al.* Psychotic Experiences in Schizophrenia and Sensitivity to Sensory Evidence. *Schizophrenia bulletin* **46**, 927–936 (2020).

1044 18. Weilnhammer, V. *et al.* An active role of inferior frontal cortex in conscious experience. *Current Biology* **31**, 2868–2880.e8 (2021).

1045 19. Manassi, M. *et al.* Continuity fields enhance visual perception through positive serial dependence. *Nature Reviews Psychology* **3**, 352–366 (2024).

1046 20. Shergill, S. S. *et al.* Evidence for sensory prediction deficits in schizophrenia. *The American Journal of Psychiatry* **162**, 2384–2386 (2005).

1047 21. Mertens, Y. L. *et al.* The Clinician-Administered Dissociative States Scale (CADSS): Validation of the German Version. *Journal of Trauma & Dissociation* **23**, 366–384 (2022).

1048 22. Kucyi, A. *et al.* Spontaneous default network activity reflects behavioral variability independent of mind-wandering. *Proceedings of the National Academy of Sciences* **113**, 13899–13904 (2016).

1049 23. Yamashita, A. *et al.* Variable rather than extreme slow reaction times distinguish brain states during sustained attention. *Scientific Reports* **11**, 14883 (2021).

1050 24. Weilnhammer, V. *et al.* Dynamic predictive templates in perception. *Current Biology* **0**, (2024).

1051 25. Muckli, L. *et al.* Contextual Feedback to Superficial Layers of V1. *Current Biology* **25**, 2690–2695 (2015).

1052 26. Notredame, C.-E. *et al.* What visual illusions teach us about schizophrenia. *Frontiers in integrative neuroscience* **8**, 63 (2014).

1053 27. Schmack, K. *et al.* Striatal dopamine mediates hallucination-like perception in mice. *Science (New York, N.Y.)* **372**, eabf4740 (2021).

1054 28. Jardri, R. *et al.* Experimental evidence for circular inference in schizophrenia. *Nature Communications* **8**, 14218 (2017).

29. Morgan, C. J. A. *et al.* Ketamine use: A review. *Addiction (Abingdon, England)* **107**, 27–38 (2012).

30. Adams, R. A. *et al.* The computational anatomy of psychosis. *Frontiers in psychiatry* **4**, 47 (2013).

31. Peters, E. R. *et al.* Measurement of delusional ideation in the normal population: Introducing the PDI (Peters et al. Delusions Inventory). *Schizophrenia bulletin* **25**, 553–76 (1999).

32. Bell, V. *et al.* The Cardiff Anomalous Perceptions Scale (CAPS): A New Validated Measure of Anomalous Perceptual Experience. *Schizophrenia Bulletin* **32**, 366–377 (2006).

33. Overall, J. E. *et al.* The Brief Psychiatric Rating Scale. *Psychological Reports* **10**, 799–812 (1962).

34. Brainard, D. H. The Psychophysics Toolbox. *Spatial vision* **10**, 433–6 (1997).

35. Dittrich, A. *et al.* 5D-ABZ: Fragebogen zur Erfassung Aussergewöhnlicher Bewusstseinszustände. *Eine kurze Einführung. PSIN Plus, Zürich* (1999).

36. Kay, S. R. *et al.* The positive and negative syndrome scale (PANSS) for schizophrenia. *Schizophrenia bulletin* **13**, 261–76 (1987).

37. Keane, B. P. *et al.* Reduced depth inversion illusions in schizophrenia are state-specific and occur for multiple object types and viewing conditions. *Journal of abnormal psychology* **122**, 506–512 (2013).

38. Silverstein, S. *et al.* Reduced Sensitivity to the Ebbinghaus Illusion is State Related in Schizophrenia. *Journal of Vision* **13**, 1261–1261 (2013).

39. Pastukhov, A. *et al.* Believable change: Bistable reversals are governed by physical plausibility. *Journal of vision* **12**, 17 (2012).

40. Weilnhammer, V. *et al.* A predictive coding account of bistable perception - a model-based fMRI study. *PLOS Computational Biology* **13**, e1005536 (2017).

41. Fleming, S. M. *et al.* How to measure metacognition. *Frontiers in Human Neuroscience* **8**, 443 (2014).

42. Linderman, S. *et al.* SSM: Bayesian Learning and Inference for State Space Models. (2020).